




Article

Development and Application of a Mechanistic Nutrient-Based Model for Precision Fish Farming

Filipe M. R. C. Soares¹, Ana M. D. Nobre¹, Andreia I. G. Raposo^{1,2}, Rodrigo C. P. Mendes^{1,3}, Sofia A. D. Engrola³ , Paulo J. A. P. Rema^{4,5} , Luís E. C. Conceição^{1,*}  and Tomé S. Silva¹

¹ Sparos Lda., Área Empresarial de Marim, Lote C, 8700-221 Olhão, Portugal

² Instituto de Ciências Biomédicas Abel Salazar (ICBAS-UP), Universidade do Porto, Rua de Jorge Viterbo Ferreira 228, 4050-313 Porto, Portugal

³ Centre of Marine Sciences, CCMAR, University of Algarve, 8005-139 Faro, Portugal

⁴ CIIMAR—Interdisciplinary Centre of Marine and Environmental Research, University of Porto, Novo Edifício do Terminal de Cruzeiros de Leixões, Avenida General Norton de Matos, s/n, 4450-208 Matosinhos, Portugal

⁵ Departamento de Zootécnia, Universidade de Trás-os-Montes e Alto Douro, Quinta de Prados, 5001-801 Vila Real, Portugal

* Correspondence: luisconceicao@sparos.pt; Tel.: +351-289435145

Abstract: This manuscript describes and evaluates the FEEDNETICS model, a detailed mechanistic nutrient-based model that has been developed to be used as a data interpretation and decision-support tool by fish farmers, aquafeed producers, aquaculture consultants and researchers. The modelling framework comprises two main components: (i) *fish model*, that simulates at the individual level the fish growth, composition, and nutrient utilization, following basic physical principles and prior information on the organization and control of biochemical/metabolic processes; and (ii) *farm model*, that upscales all information to the population level. The model was calibrated and validated for five commercially relevant farmed fish species, i.e., gilthead seabream (*Sparus aurata*), European seabass (*Dicentrarchus labrax*), Atlantic salmon (*Salmo salar*), rainbow trout (*Oncorhynchus mykiss*), and Nile tilapia (*Oreochromis niloticus*), using data sets covering a wide range of rearing and feeding conditions. The results of the validation of the model for fish growth are consistent between species, presenting a mean absolute percentage error (MAPE) between 11.7 and 13.8%. Several uses cases are presented, illustrating how this tool can be used to complement experimental trial design and interpretation, and to evaluate nutritional and environmental effects at the farm level. FEEDNETICS provides a means of transforming data into useful information, thus contributing to more efficient fish farming.

Keywords: aquaculture; fish nutrition; precision fish farming; mechanistic nutrient-based model; numerical model; decision-support tool



Citation: Soares, F.M.R.C.; Nobre, A.M.D.; Raposo, A.I.G.; Mendes, R.C.P.; Engrola, S.A.D.; Rema, P.J.A.P.; Conceição, L.E.C.; Silva, T.S. Development and Application of a Mechanistic Nutrient-Based Model for Precision Fish Farming. *J. Mar. Sci. Eng.* **2023**, *11*, 472. <https://doi.org/10.3390/jmse11030472>

Academic Editors: Ana Catarina Matias and Carlos Andrade

Received: 16 January 2023

Revised: 20 February 2023

Accepted: 21 February 2023

Published: 22 February 2023



Copyright: © 2023 by the authors. Licensee MDPI, Basel, Switzerland. This article is an open access article distributed under the terms and conditions of the Creative Commons Attribution (CC BY) license (<https://creativecommons.org/licenses/by/4.0/>).

1. Introduction

As fish farming is becoming more digitized, data analytics tools are required to transform data into useful information. Mathematical models that are able to describe and predict the dynamics of fish farming systems are candidate tools in this regard, with great potential to contribute as data interpretation and decision support tools [1,2].

Over the last decades, several mathematical models that describe the state of fish have been developed to support fish farming operations [3–9]. Some models describe the growth of fish based on simple empirical equations that assume that feeding is a non-limiting factor, and is therefore not included as a model input [8,10–15]. Others, based on differential equations, describe the growth and, in some cases, the composition of fish (among other indicators), given time-dependent information about environmental parameters (e.g., water temperature) and feeding operations (e.g., ration size, feed composition) [3,6,16–18].

For a more detailed description of different models that describe fish growth and body composition, see the reviews from Dumas et al. [7] and Chary et al. [9].

Usually, the choice of one type of model over another strongly depends on the availability of data and the purpose for which the model is intended. Within the framework of precision fish farming [1], where highly detailed information systems are required to support a knowledge-based decision-making process, the use of more detailed mathematical models as complementary tools to simpler models may open the door to new insight. For example, detailed mathematical models that account for the effects of ration size and feed composition (e.g., bioenergetic or nutrient-based models) can be used to quantify the impact of different feed formulations or feeding strategies on fish performance, allowing to pre-screen the most promising solutions before practical application [19]. Besides, this type of models can also be used to monitor and predict on a higher time resolution basis (e.g., hourly or daily basis) the state of production using data from past observations and data defining the expected environmental and feeding conditions of the farming unit. Having access to this additional information allow fish farmers to make more informed decisions based on the specific conditions of their farms, and on the current and future state of production; e.g., estimate feed requirements, manage feed stocks, detect disease outbreaks, and plan sales and harvesting dates [16–18,20–22].

Nutrient-based models—defined here as models that explicitly describe the nutritional state of fish based on nutrient intake and utilization—enable a quantitative prediction of the effects of feed composition, in terms of macronutrients, on fish performance [19,23]. This is a particularly relevant aspect, as the range of commercially available feeds for each growth stage can differ in composition. Besides, since feeds with the same energy content may present different nutrient composition, consequently inducing different fish performance [24–26], the use of nutrient-based models may be preferable to bioenergetic models. Within the domain of nutrient-based models, a relevant aspect to be considered is the level of detail included in the modelling approach. Simpler nutrient-based models (also known as “nutrient mass-balance models”) that only consider the protein and energy content of the feed are not able, for example, to predict the impact of imbalanced dietary amino acid profiles on fish performance [18]. To work with greater precision, it is therefore necessary to use mechanistic nutrient-based models (also known as “metabolic-flux models”) that account for the effects of the feed amino acid profile and that describe the main physiological and metabolic processes of fish (e.g., protein synthesis and degradation, amino acid oxidation and conversion, glycolysis, gluconeogenesis, glycogenesis, and glycogenolysis).

A few detailed mechanistic nutrient-based models of fish have been previously developed by other authors [3–6,19,23,27,28]. For example, Bar et al. [23] developed a highly detailed model of nutrient-pathways, growth, and body composition of fish, calibrated for Atlantic salmon (*Salmo salar*), that considers the effects of limiting amino acids. In turn, Hua et al. [19] adapted a non-ruminant nutrient-based model for rainbow trout (*Oncorhynchus mykiss*), which explicitly describes the utilization of energy-yielding nutrients and metabolites for protein and lipid deposition in the fish body, also considering the effects of limiting amino acids. These previous works set solid foundations that can be further explored to advance on the development of more detailed mechanistic nutrient-based models of fish growth and composition.

This manuscript presents the FEEDNETICS model, a detailed mechanistic nutrient-based model that has been developed to be used as a data interpretation and decision-support tool in the context of precision fish farming. This tool has a wide range of potential applications and it is aimed at fish farmers, aquafeed producers, aquaculture consultants and researchers. The main objectives of this work were:

1. To develop a nutrient-based model that considers the main physiological and metabolic processes of fish;
2. To calibrate and validate the model for five relevant farmed fish species, i.e., gilthead seabream (*Sparus aurata*), European seabass (*Dicentrarchus labrax*), Atlantic salmon (*Salmo salar*), rainbow trout (*Oncorhynchus mykiss*), and Nile tilapia (*Oreochromis niloticus*);

- To demonstrate the use of the model as a data interpretation and decision-support tool through several use cases.

2. Materials and Methods

2.1. Model Description

FEEDNETICS is a dynamic mechanistic nutrient-based model that simulates fish growth, composition and environmental impact, within the context of fish farming operations, while following basic physical principles (e.g., energy and mass conservation) and prior information on the organization and control of biochemical/metabolic processes. It deterministically simulates the time-dependent physiology and metabolism of a single fish (the “average fish”; *fish model*), being driven by temperature data, feed properties and quantity, which is then upscaled to a population of fish (*farm model*). Figure 1 shows an overview of the input data needed to run the model and the output data it provides.

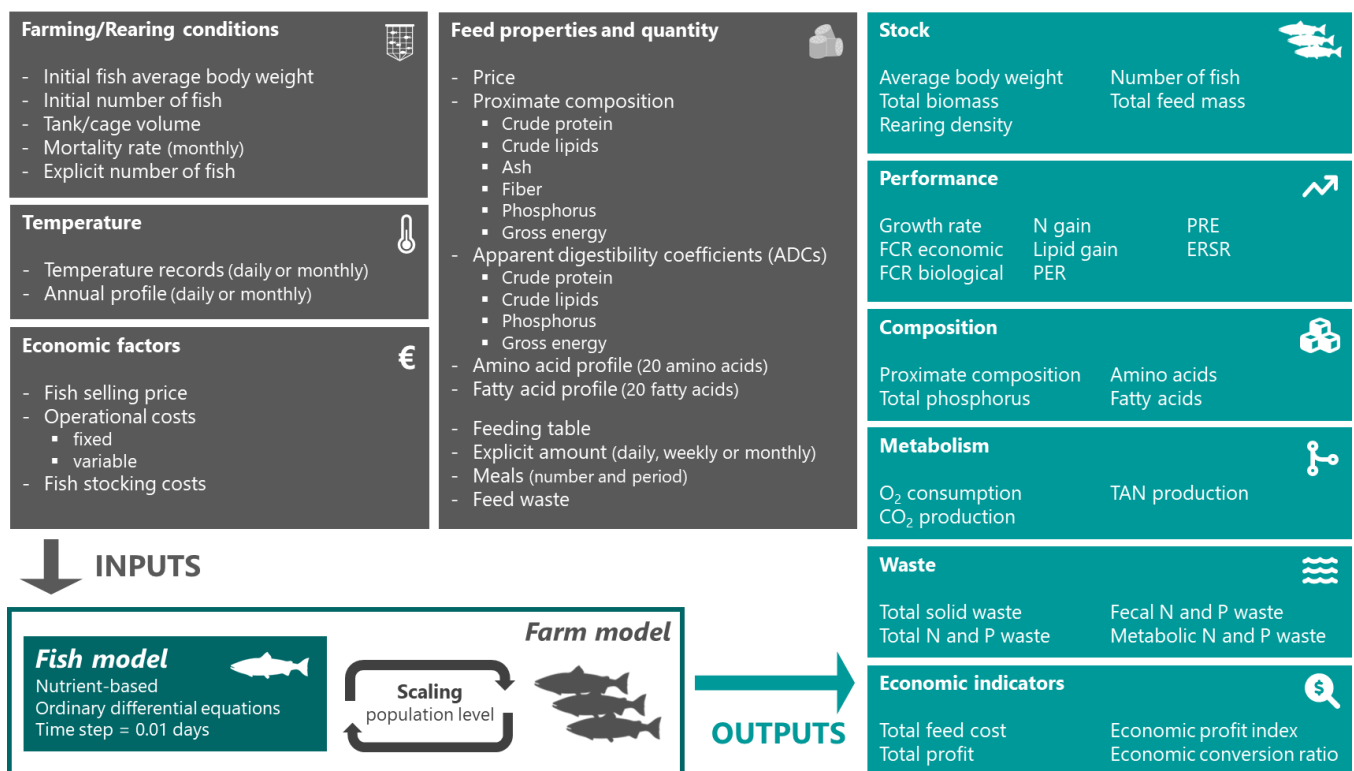


Figure 1. Diagram illustrating the main model inputs and outputs.

In particular, the model considers the most relevant physiological and metabolic processes, including feed intake, digestion, nutrient absorption and transport, central metabolism (i.e., glycolysis, gluconeogenesis, glycogenesis, glycogenolysis, beta-oxidation of fatty acids, Krebs cycle) and nitrogen metabolism (i.e., protein synthesis, protein degradation, synthesis of non-essential amino acids, amino acid oxidation, amino acid conversion) in order to maximize its capability to effectively predict fish body weight and composition along time for general scenarios. A detailed description of this model is provided in Appendix A.

The model has been implemented as a set of difference equations in the Powersim Studio 10 Expert software (Powersim Software AS, Nyborg, Norway), which are solved numerically through forward Euler integration with a fixed timestep of 0.01 days.

2.2. Model Calibration and Validation

The model was calibrated and validated for five fish species: gilthead seabream, European seabass, Atlantic salmon, rainbow trout, and Nile tilapia. The data sets used to

calibrate and validate the model, as well as the calibration and validation procedures, are described below.

2.2.1. Data Processing and Data Sets Description

All data sets used in this work include data about several *in vivo* growth trials, covering a wide range of rearing and feeding conditions (see Table 1). Those were collected from the scientific literature and from data generated by Sparos Lda., and its partners, in R&D projects, some of which were specifically designed to support model calibration and validation.

Table 1. Overview of the data used to calibrate and validate the model for each species.

Attributes	Unit	Gilthead Seabream	European Seabass	Atlantic Salmon	Rainbow Trout	Nile Tilapia
Nr. of data sources	-	19	37	61	33	44
Nr. of observational units	-	118	126	398	110	186
Nr. of diets	-	30	66	350	58	175
Body weight range	g	1–478	5–482	1–6645	2–2080	1–559
Temperature range	°C	11–28	18–26	4–20	4–19	18–30
Diet composition range						
Crude protein	% as fed	37–58	37–56	29–54	26–58	23–46
Crude lipids	% as fed	9–23	10–31	10–47	6–31	3–15
Gross energy	MJ/kg	19–23	18–25	18–29	17–26	13–21
DP/DE	g/MJ	21–26	19–30	12–26	11–28	14–26

For purposes of uniformization and data handling, all data sets were processed into a standard format and stored in a database structured according to ‘tidy data’ principles [29]. Three types of data are associated to each data set (Figure 2):

- *Raw data*: data in the exact same format/structure as it was collected from the data source;
- *Processed data*: processed data stored in a standard format, where each observational unit is a table (representing a tank or cage), each attribute is a column (including responses and covariates), and each observation is a row (numerical data that describe the state of the observational unit over time, on a daily resolution basis);
- *Metadata*: data that describe the main characteristics of each data set.

During data processing, different methods were applied to convert the *raw data* into *processed data*, including the use of simple conversion factors (e.g., to convert whole-body composition and diet composition from dry weight to wet weight, and to calculate the energy content of diets), linear and non-linear interpolation methods (e.g., to distribute feed intake and temperature data over time, on a daily resolution basis, whenever the data source provided aggregated information), and additive models (e.g., to estimate the dietary amino acid profile and apparent digestibility coefficients based on ingredient composition). In addition, in cases where it was not possible to apply these methods, default values per species were used to ensure that all the minimum required attributes were defined.

After data processing, all *processed data* sets were subjected to quality analysis (e.g., comparison of diet proximate composition and fish whole-body composition data against realistic bounds; analysis of zootechnical indicators, namely nutrient retention efficiencies) in order to identify potential flaws in the data and remove outliers. The different data sets were then partitioned into calibration and validation data sets (roughly 80% for calibration and 20% for validation), based on *metadata* attributes. This process was performed ensuring that the calibration and validation data sets included data covering similar ranges of experimental conditions.

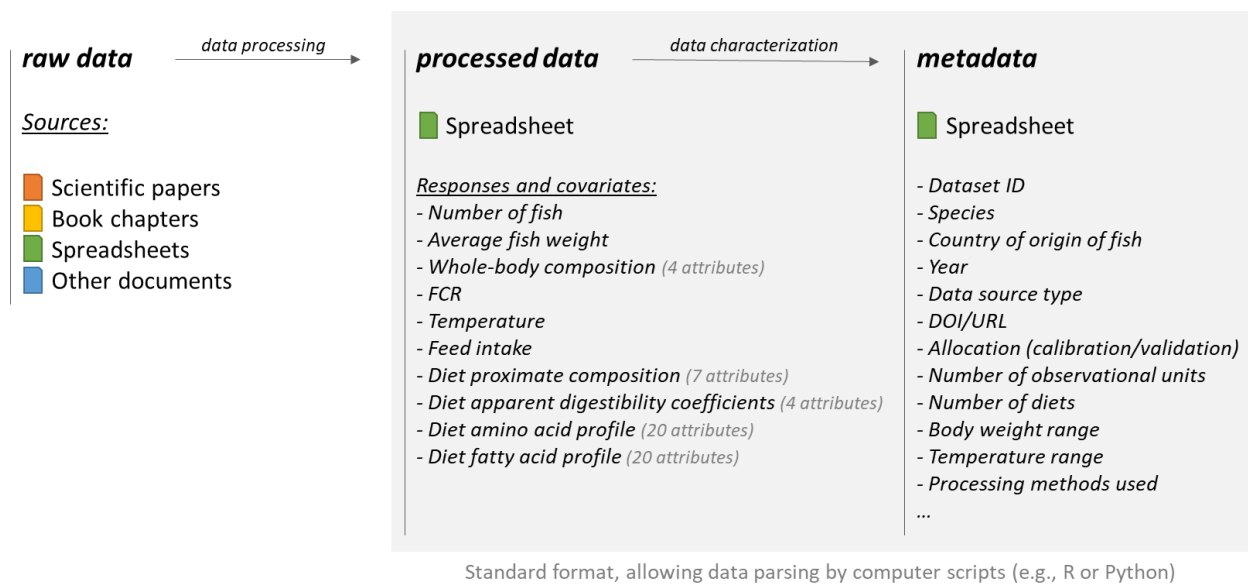


Figure 2. Diagram describing the data set structure, comprising three types of data: *raw data*, *processed data*, and *metadata*.

2.2.2. Model Calibration

For each species, the model was calibrated using the data sets allocated for calibration purposes, in a two-step approach.

In a first step, a subset of model parameters was statically calibrated. This process included the use of linear regression techniques (e.g., least squares, Huber loss minimization, quantile regression) to calibrate body composition and feed intake models, and the assignment of published values to constant or quasi-constant biochemical attributes (e.g., fatty acid molecular weights, energy conversion factors, whole-body amino acid profile).

In a second step, the remaining model parameters were dynamically calibrated in the Powersim Studio 10 Expert software (Powersim Software AS, Nyborg, Norway), using an evolutionary optimization algorithm based on the CMA-ES (covariance matrix adaptation evolutionary strategy) approach [30]. This process comprised the specification of general settings related to the evolutionary algorithm (i.e., number of generations, parents and offspring), the selection of a set of decisions (i.e., model parameters to be calibrated), the adjustment of the calibration space (i.e., minimum and maximum values allowed for each parameter), and the definition of the target set of objectives (weighted loss functions; i.e., $MAPE_{calbw}$ weighing 10.00, CAE_{bw} weighing 0.01, and WE_{CL} weighing 0.10). The following Equations (1)–(3) describe the loss functions:

$$MAPE_{calbw}(\%) = \frac{100}{n} \sum_{i=1}^n \left| \frac{P_{bwi} - O_{bwi}}{O_{bwi}} \right|, \tag{1}$$

$$CAE_{bw}(g) = \sum_{i=1}^n |P_{bwi} - O_{bwi}|, \tag{2}$$

$$WE_{CL} = \frac{1}{m} \sum_{j=1}^m \left(CL_{ref} - CL_{predicted} \right)^2 \times 0.1, \tag{3}$$

where $MAPE_{calbw}$ is the body weight mean absolute percentage error, CAE_{bw} is the body weight cumulative absolute error, n is the number of predicted-observed value pairs, P_{bwi} is the predicted body weight value (g), O_{bwi} is the observed body weight value (g), WE_{CL} is the crude lipids weighted error, $CL_{predicted}$ is the predicted whole-body crude lipids content (%), CL_{ref} is a reference value for whole-body crude lipids content (%) derived from quantile regression of body composition data, and m is the number of time steps.

Model calibration was run until the evolutionary optimization algorithm reached the minimum convergence rate or limit of generations specified, in order to find a plausible parameterization that minimizes the prediction error for the calibration data set.

2.2.3. Model Validation

For each species, the model was validated using the independent data sets allocated for validation purposes (i.e., *processed data* files not used for model calibration). The validation results were evaluated qualitatively, through visual inspection of the model behavior over time in comparison with point observations, and quantitatively, by estimating the body weight mean absolute percentage error for the validation data set ($MAPE_{valbw}$) (4), as follows:

$$MAPE_{valbw}(\%) = \frac{100}{n} \sum_{i=1}^n \left| \frac{P_{bwi} - O_{bwi}}{O_{bwi}} \right|, \quad (4)$$

where n is the number of predicted-observed value pairs, P_{bwi} is the predicted body weight value (g), and O_{bwi} is the observed body weight value (g).

2.3. Model Application

Various applications are presented to illustrate the use of the model to complement experimental trial design and interpretation, and to support the aquaculture industry in evaluating the impact of nutritional and environmental effects at the farm level.

2.3.1. Complement Trial Design and Interpretation

The experiment conducted by dos Santos et al. [31] aimed to evaluate the performance of different Nile tilapia strains (i.e., GIFT-1, GST-24, GIFT-2, GST-14) reared under similar conditions. The authors used the Gompertz model (sigmoid function) as a tool to support the analysis of the results, namely, to characterize the growth pattern and growth rate of the different strains evaluated. The nutrient-based model presented here can be used to further complement the analysis of the results. In particular, and because the model includes feeding as an input, it provides a method to ascertain if the differences in weight gain are due to differences in feed intake. To this end, we ran the model considering as inputs data made available by dos Santos et al. [31] in the published version of the article (i.e., initial weight, temperature, FCR), as well as other additional information provided by the main author (personal communication; i.e., feeding rates and diet proximate composition). The results of the model were compared with the experimental results to make further inferences about the performance of the aforementioned Nile tilapia strains.

Additionally, we considered the experiment presented by Farinha et al. [32], which focused on the evaluation of European seabass juveniles that were fed diets with varying methionine levels. To formulate the diets and define the methionine levels to be considered, the authors relied on the findings of a previous study carried out with similar diets and with fish of about the same size. The nutrient-based model presented here was applied to this study to show how it could have contributed as a complementary tool to support the design of the experiment, namely, in defining the different methionine levels to be tested. This illustrates the usefulness of the model for cases where there are no previous scientific findings available to support the design of the experiment. To this end, we ran the model considering as inputs the detailed records of the experiment presented by Farinha et al. [32]. The results of the model were compared with experimental data to illustrate the model's ability to predict the growth of European seabass when fed diets with varying methionine levels.

2.3.2. Evaluate Nutritional and Environmental Effects at the Farm Level

To demonstrate further uses of the model by the industry, three distinct use cases are made available in Appendix B:

1. Use case 1: Evaluate the impact of different commercial feeds on trout production performance;

2. Use case 2: Evaluate the impact of different temperature profiles on post-smolt production performance;
3. Use case 3: Predict the long-term effects of marginal changes in diet digestibility on bream production performance.

These model applications were carried out considering typical fish farming production scenarios, generally using information at the level that is available to the typical user (e.g., diet composition and feeding rates were defined based on information available in official technical sheets provided by feed producers). In each application, the different scenarios were evaluated by comparing several key-performance indicators provided by the model (e.g., time to reach harvest weight, growth rate, feed conversion ratio—FCR, economic conversion ratio—ECR).

3. Results

3.1. Model Calibration and Validation

3.1.1. Model Performance for Calibration Data Sets

Table 2 presents the final estimates of the three loss functions (error metrics) used to dynamically calibrate the model for each species (i.e., $MAPE_{calbw}$, CAE_{bw} and WE_{CL} ; see Equations (1)–(3) for formulas).

Table 2. Error metrics for the calibration data set for each species.

Loss Functions/Error Metrics	Gilthead Seabream	European Seabass	Atlantic Salmon	Rainbow Trout	Nile Tilapia
$MAPE_{calbw}$ (%)	6.82	5.15	6.33	8.28	18.18
CAE_{bw} (g)	91.29	75.70	588.83	162.12	166.04
WE_{CL} (–)	0.24	0.16	0.17	0.27	0.20

Overall, the performance of the model in predicting the body weight of fish for the calibration data sets is similar for most fish species in terms of $MAPE_{calbw}$. However, it must be pointed out that the model presents worse performance for Nile tilapia ($MAPE_{calbw} = 18.18\%$) compared to other species ($MAPE_{calbw}$ between 5.15% and 8.28%).

The worse performance for Nile tilapia may be related to several reasons linked to the data sets of this species, two of which are worth mentioning: (i) the different publications on the experiments carried out with Nile tilapia appear to show a much greater variability in terms of rearing conditions (e.g., rearing density, water quality) than the other species, which may explain part of the deviation between model predictions and observations; and (ii) the high variability of Nile tilapia strains used in different studies can also contribute to the higher calibration error in Nile tilapia, since, if the differences between strains are manifested in different metabolic rates or nutrient utilization efficiencies, those differences may not be fully replicated by the current model parametrization as the model calibration was done at the species level and not at the strain level.

The CAE_{bw} and WE_{CL} directly depend on the size, structure, and content of the calibration data set; therefore, they are presented here for reference only and not used to make any considerations about the model performance.

Given the outcomes of the calibration procedure, the resulting parameter sets were accepted and used for the model validation stage.

3.1.2. Model Performance for Validation Data Sets

Figure 3 shows the model validation results for each species in terms of body weight prediction. In general, the model accuracy is consistent across species, presenting a mean absolute percentage error ($MAPE_{valbw}$) ranging between 11.7% and 13.8%. The relative error distribution shows a symmetrical pattern, meaning that the scale and sign of model deviations are homogeneous over the body weight range (i.e., there is no clear bias for under- or over-estimation). The higher density of points for lower body weight classes

(more evident in the case of rainbow trout due to higher n), is explained by the fact that most of the data sets used to validate (and calibrate) the model for each species are related to experiments carried out with small fish.

Visual inspection of the model behavior over time indicates that the predictions are representative of the observed growth pattern of fish (see Section 3.2. Model Application for examples). However, as expected, for some validation data sets, the magnitude of the deviation between model predictions and observations tends to increase throughout the simulation, since simulation errors are cumulative and generally multiplicative, and the model is not re-initialized when there are intermediate sampling points.

It is also worth mentioning that, although $MAPE_{valbw}$ can be seen as a proxy for the model generalization error, one cannot always expect an accuracy according to this error metric when extrapolating fish growth with this model. Model accuracy is not only dependent on the model itself, but also on the quality of the input data used to drive it. Thus, in order to obtain accurate predictions, we cannot fail to mention that the input data used to drive the model must be as representative as possible of the scenarios to be evaluated.

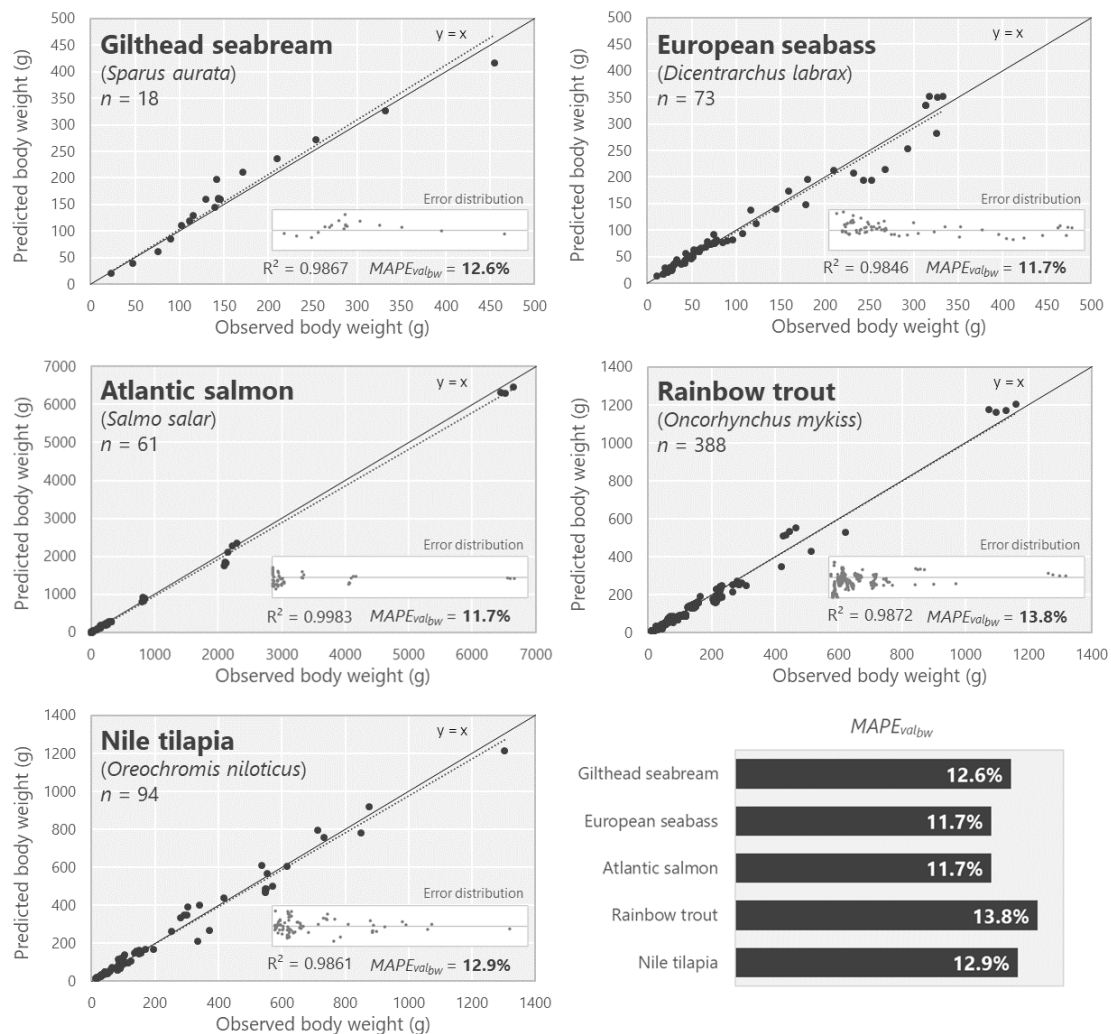


Figure 3. Scatter plots showing predicted versus observed body weight for the validation data set of each species, where n is the number of predicted-observed value pairs and $MAPE_{valbw}$ is the mean absolute percentage error. The solid line denotes the line of equality ($y = x$) and the dotted line is the linear trendline. Inside each plot, in a smaller frame, is shown the relative error (y -axis) distributed over the body weight range (x -axis). On the lower-right corner, a bar plot shows a comparison between the $MAPE_{valbw}$ values obtained for the different species.

3.2. Model Application

3.2.1. Complement Trial Design and Interpretation

Figure 4 shows the time series of predicted and observed average body weight values for the dos Santos et al. [31] data set, which includes data about different Nile tilapia strains (i.e., GIFT-1, GST-24, GIFT-2, GST-14) reared under similar conditions. For all Nile tilapia strains, the model predictions for body weight are consistent with the observations, with a MAPE ranging between 11.4% and 16.9%. The predicted relative growth rate (RGR, %/day) is also in line with the observed values.

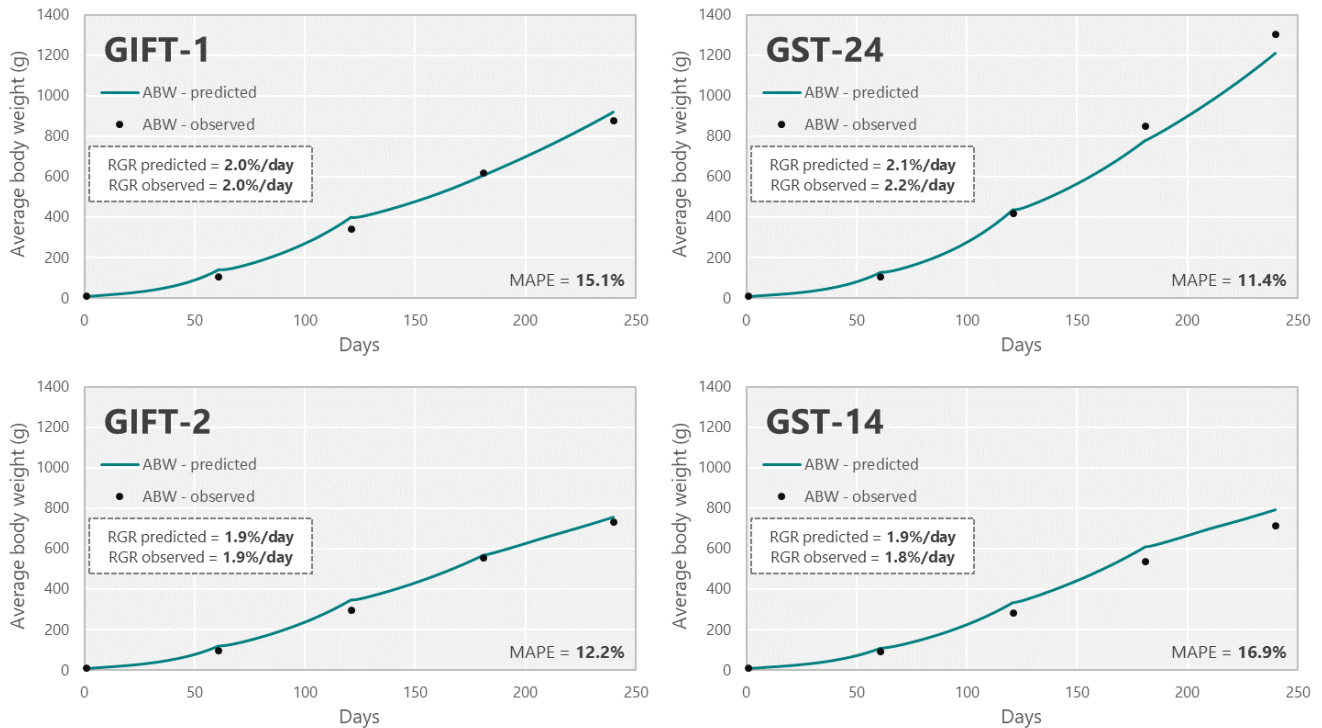


Figure 4. Time series of predicted (solid line) and observed (points) average body weight (ABW) for the dos Santos et al. [31] data set, which includes experimental data about different Nile tilapia strains (i.e., GIFT-1, GST-24, GIFT-2, GST-14) reared under similar conditions. MAPE stands for mean absolute percentage error (%) and RGR for relative growth rate (%/day), the latter calculated as: $RGR = \left(e^{(\ln(ABW_{i+n}) - \ln(ABW_i)) / (day_{i+n} - day_i)} - 1 \right) \times 100$.

The ability of the model to predict the growth of these four strains suggests that differences in the growth performance of these strains are mainly related to feed intake, i.e., higher growth rates were achieved due to the capacity of some strains (i.e., GST-24 and GIFT-1) to ingest more feed. This is something that is not apparent when analyzing the experimental data or the results from simpler growth models, such as the Gompertz model, and that can complement the research presented by dos Santos et al. [31]. If differences in growth performance were manifested due to different metabolic efficiencies, the nutrient-based model should clearly reflect this, by predicting the growth of some strains expressively better than others, over the entire period. Information about the observed voluntary feed intake (VFI, % body weight/day; GIFT-1 = 5.92%/day, GST-24 = 6.45%/day, GIFT-2 = 5.33%/day, GST-14 = 5.64%/day) also indicate a direct positive relationship between feed consumption and growth rate. However, these values alone do not support the hypothesis that the main factor driving growth performance is feed intake capacity, since this indicator does not aggregate information on the nutrient utilization capacity. This application illustrates how this nutrient-based model can be a useful tool to support the interpretation of experimental results, contributing to new insights about the main factors that explain fish performance.

Figure 5 shows the time series of predicted and observed average body weight values for the Farinha et al. [32] data set, which includes experimental data about European seabass that were fed diets with different methionine levels (i.e., M0.65, M0.85, M1.25, M1.50). For all dietary treatments, the model predictions are consistent with the observations, with a MAPE ranging between 2.6% and 11.5%. This means that the model is able to predict the effects of different methionine levels on the growth performance of European seabass accurately.

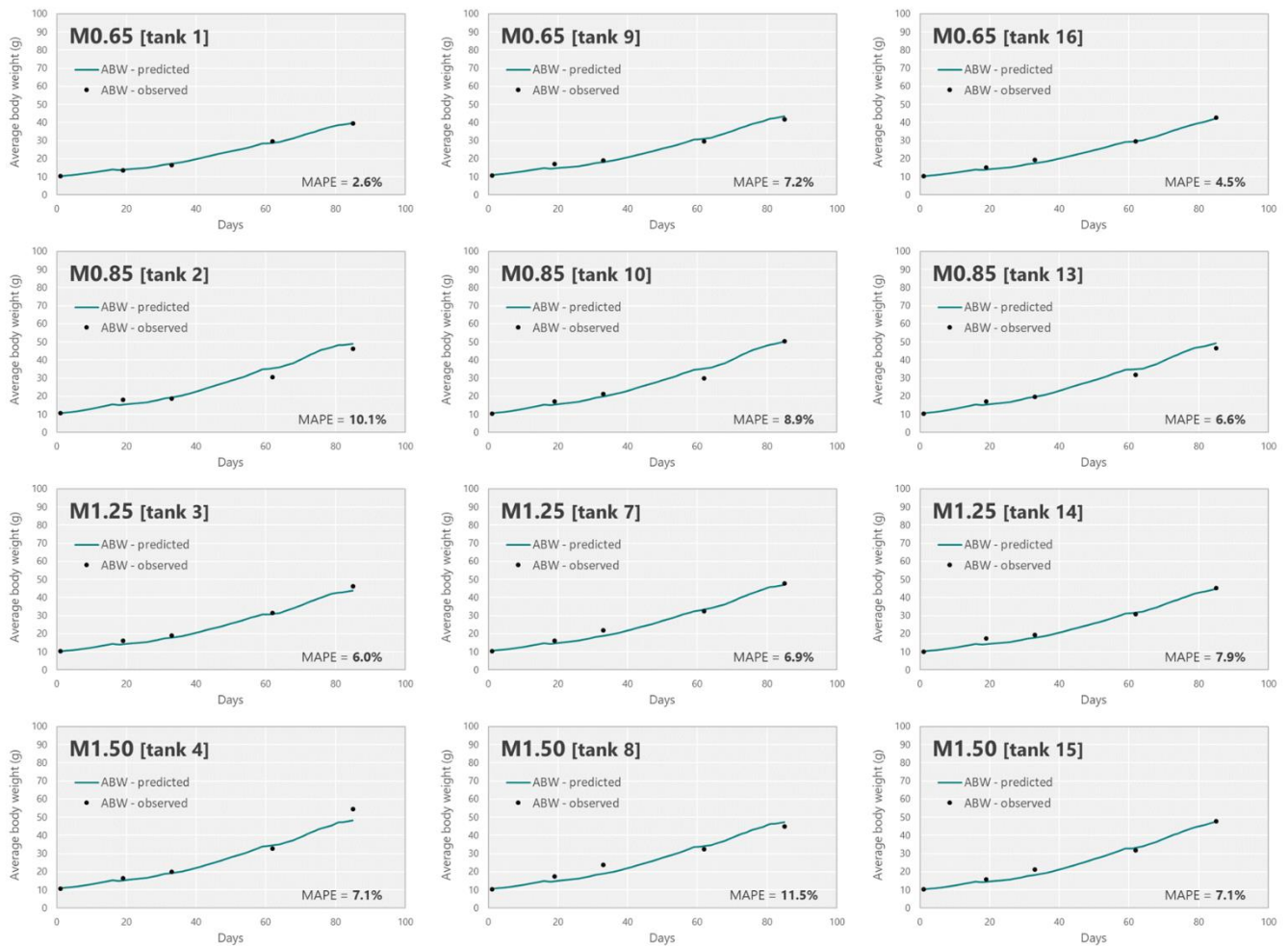


Figure 5. Time series of predicted (solid line) and observed (points) average body weight (ABW) for the Farinha et al. [32] data set, which includes experimental data about European seabass that were fed diets with different methionine levels (i.e., M0.65, M0.85, M1.25, M1.50). MAPE stands for mean absolute percentage error (%).

As described by Farinha et al. [32], the analysis of experimental data through one-way ANOVA indicated significant differences between the dietary treatments M0.65 and M1.50 for final average body weight, pointing to methionine deficiency in fish fed with the M0.65 diet. The authors further carried out a linear broken-line regression analysis to find the breakpoint that defines the methionine level below which growth performance is affected (i.e., methionine requirement). Usually in this type of assessment (broken-line regression), it is recommended (not mandatory though) to have at least two observed points in each segment so as to ensure that the slope of each segment is estimated based on points directly related to observed data and that the breakpoint is then defined with better precision. However, this was something that did not happen, as M0.65 was the only diet that displayed a clear methionine deficiency, meaning that the broken-line was adjusted considering only one directly observed point below the breakpoint. The use of the

nutrient-based model presented in this work could have been useful during the design of this experiment as it could have allowed a better definition of the methionine levels to be tested (prescreening of diets *in silico*), in order to ensure at least two points (methionine levels) below the breakpoint. This illustrates how this nutrient-based model can be a useful tool to support the design of experiments, helping to anticipate fish performance, and thus, make more informed decisions to ensure full effectiveness of the experiment to be performed. Furthermore, in nutrient requirements studies similar to the one presented by Farinha et al. [32], the model can also be used to extrapolate the performance of fish subjected to different rearing conditions (e.g., different temperatures) or diet compositions (e.g., different protein or energy content) to verify whether the nutrient requirements determined apply in those cases or not.

3.2.2. Evaluate Nutritional and Environmental Effects at the Farm Level

Additional model applications directed to industrial end users (e.g., fish farmers, aquafeed producers, and aquaculture consultants) are presented in Appendix B and include the following use cases: 1. evaluate the impact of different commercial feeds on trout production performance; 2. evaluate the impact of different temperature profiles on post-smolt production performance; and 3. predict the long-term effects of marginal changes in diet digestibility on bream production performance. These applications illustrate how the nutrient-based model presented here can be used as a decision-support tool, helping to define the best feeding and farming strategies for each specific case, through the analysis of the impact of nutritional and environmental effects at the farm level.

4. Discussion

This manuscript describes and evaluates the FEEDNETICS model, a mechanistic nutrient-based model intended to be used as a data interpretation and decision-support tool by different end users, i.e., fish farmers, aquafeed producers, aquaculture consultants, and researchers. The framework behind FEEDNETICS comprises two main components: (i) *fish model*, that simulates at the individual level the fish growth, composition, and nutrient utilization, and (ii) *farm model*, that upscales all information to the population level.

The *fish model* is based upon a mechanistic and deterministic modelling approach, following basic physical principles and prior information on the organization and control of biochemical/metabolic processes. It assumes a multi-compartmental structure describing the flow of nutrients and metabolites between the gut, blood, and body (single compartment representing the main body tissues, e.g., brain, liver, muscle, adipose tissue, bone). Similar mechanistic nutrient-based models have been previously developed by other authors for larval [6,28], juvenile, and adult fish stages [3–5,19,23,27]. However, not all of these models explicitly consider different compartments to describe the flow of nutrients and metabolites. Although not a requisite to predict the growth and body composition of fish, assuming a multi-compartmental structure enables a more realistic description of nutrient flow and utilization rates. In addition, its modular nature facilitates the continuous improvement of the model through the simplification or complexification of specific (sub-)processes. For example, in the current version of the model, the *gut* compartment does not mechanistically simulate the digestive process, since the apparent digestibility coefficients (ADCs) of nutrients are provided as input. However, as nutrient digestibility of feeds may vary with fish size, water temperature, and ration size [33–37], among other factors, it may be relevant to refine the model in order to account for such effects. As the gut is considered as a separate compartment in this model, future improvements aimed at incorporating a mechanistic description of the digestive process can be achieved without the need to completely reformulate the entire structure of the model. The same is applicable to other physiological and metabolic processes (e.g., appetite and ingestion).

The *farm model* was implemented based on the assumption that the entire fish population can be described based on a linear scaling of the outputs provided by the *fish model*. Therefore, the existing inter-individual variability is not accounted for in the current model

implementation. Although it is a strong assumption, this approach aims to simplify the required input data from the user. Furthermore, it must be pointed out that accurately modelling fish size distribution within a population is challenging, as it is not only affected by genetic variability among individuals, but may also be influenced by production practices (e.g., ration size and stocking density) [38–40]. Nevertheless, if relevant for future applications, some outputs provided by the *farm model* can be modified in order to scale from individual to population level based on fish size distribution functions, where the parameters of such functions would be considered as input.

In general terms, and despite the simplifications that were assumed to ensure greater usability, the model has a complex and detailed structure. Considering such a high level of detail has the advantage of making the model usable for a wider range of purposes. However, it also means that the input data needed to run the model are considerably more detailed than in the case of simpler models (e.g., bioenergetic models) [20]. While this may not be an issue for some end users (e.g., aquafeed producers, aquaculture consultants and researchers), it may compromise usability for others who may not have access to detailed information, namely in terms of the nutrient composition of feeds (e.g., fish farmers). This usability issue is highly relevant and should be considered when implementing this tool as a user-friendly application. To overcome it, it is suggested to define default values and implement auxiliary data processing methods to deal with missing input data. Default values can be defined under different assumptions, but it must be ensured that they meet the requirements of the species and that they are representative, as far as possible, of common practices applied in the industry. Auxiliary data processing methods can be implemented on top of different data structures, for example, to convert monthly resolution data to daily resolution data, or to estimate amino acids and apparent digestibility coefficients of feeds based on information about the composition of its ingredients.

The calibration and validation of the model was carried out at the species level, for five commercially relevant farmed fish species, i.e., gilthead seabream, European seabass, Atlantic salmon, rainbow trout, and Nile tilapia. In these procedures, we made use of data sets related to *in vivo* experimental trials covering a wide range of rearing and feeding conditions (see Section 2.2.1. Data Processing and Data Sets Description). Most of these data sets were collected from the scientific literature and include valuable knowledge effortfully generated over the last few decades by the academic community. Calibrating the model with these data sets means that part of this prior knowledge is being integrated through mathematical functions and made easily available to support new advances in fish farming and nutrition. The extension of the model to other species can be done following the same calibration and validation procedures, once sufficient data is collected and processed to do so. Furthermore, the model can also be calibrated in order to accommodate physiological and metabolic differences of different fish lineages/strains.

Overall, the results of the validation of the model for fish growth are consistent between species, presenting a mean absolute percentage error (MAPE) between 11.7 and 13.8%. An objective characterization of the model precision is something difficult to generalize, as the acceptable error range is often subjective and strongly depends on the application for which the model is intended to be used. Therefore, it is advisable for users to carry out more specific assessments in this regard, for example, by comparing the precision of this model for a particular application against other available methods that can be applied for the same purpose. While doing so, it is important to ensure that the input data used to run the model is representative and as accurate as possible, and that the complexity of the problem being solved is adequate for all methods being compared.

Various model applications are presented in Section 3.2. Model Application and in Appendix B. Those illustrate how the FEEDNETICS model can be used to complement trial design and interpretation and to support in the evaluation of nutritional and environmental effects at the farm level. However, the applications illustrated here represent only a small picture of the potential uses that can be made out of this model. Further potential applications include, for example, using the model to optimize finishing feeding strategies

that aim to enrich fish with a high content of omega-3 fatty acids, or using it as a monitoring and forecasting tool to provide information about the current and future state of production on a daily basis.

Future model developments can be made at several levels, some of which have already been mentioned above. The multi-compartmental structure of some physiological and metabolic processes included in the *fish model* allows simplifying or complexifying the modeling approach to improve the model's ability to describe fish performance. In addition, optimization algorithms can be implemented on top of the model to move from what-if scenario analysis to automated criteria-based optimization, where the algorithm would find the best solutions based on a set of criteria (e.g., key-performance indicators) pre-defined by the user.

5. Conclusions

In an era of increasing digitization, where it is important to transform data into useful information, the development and deployment of mathematical models as data interpretation and decision-support tools will contribute in the movement towards the implementation of precision fish farming practices. The ultimate goal is to increase production efficiency and productivity through greater knowledge and control of the systems. FEEDNETICS provides a means of transforming data into useful information, thus contributing to further advances in the fish farming industry and more efficient production.

Author Contributions: Conceptualization, T.S.S. and L.E.C.C.; methodology, T.S.S., F.M.R.C.S., A.M.D.N. and L.E.C.C.; software, T.S.S. and F.M.R.C.S.; validation, F.M.R.C.S., T.S.S. and A.M.D.N.; formal analysis, T.S.S. and F.M.R.C.S.; investigation, F.M.R.C.S., T.S.S., R.C.P.M., A.I.G.R., A.M.D.N., L.E.C.C., S.A.D.E. and P.J.A.P.R.; resources, T.S.S., F.M.R.C.S., L.E.C.C., S.A.D.E. and P.J.A.P.R.; data curation, F.M.R.C.S., T.S.S., R.C.P.M., A.I.G.R. and A.M.D.N.; writing—original draft preparation, F.M.R.C.S. and T.S.S.; writing—review and editing, F.M.R.C.S., T.S.S., A.M.D.N., L.E.C.C., R.C.P.M., A.I.G.R., S.A.D.E. and P.J.A.P.R.; visualization, F.M.R.C.S., T.S.S. and A.M.D.N.; supervision, T.S.S. and L.E.C.C.; project administration, L.E.C.C.; funding acquisition, L.E.C.C., A.M.D.N., F.M.R.C.S., T.S.S., S.A.D.E. and P.J.A.P.R. All authors have read and agreed to the published version of the manuscript.

Funding: This work results from activities on the following projects: AquaIMPACT, funded by the European Union's Horizon 2020 research and innovation program under grant agreement no. 818367; FEEDNETICS 4.0, funded by EUROSTARS-2 program, and by Portugal and the European Union through FEDER/ERDF, CRESC Algarve 2020 and NORTE 2020, in the framework of Portugal 2020 under reference E!12516-FEEDNETICS 4.0_40813; NoviFEED, funded by Iceland, Liechtenstein and Norway, through EEA grants, in the scope of the program Blue Growth, operated by the Directorate General for Maritime Policy (DGPM), Portugal, under reference PT-INNOVATION-0099; and from FCT—Foundation for Science and Technology—through projects UIDB/04326/2020, UIDP/04326/2020, and LA/P/0101/2020.

Institutional Review Board Statement: Not applicable.

Informed Consent Statement: Not applicable.

Data Availability Statement: The processed data sets used for model calibration, validation, and application are not publicly available due to proprietary and commercial use restrictions. All processed data sets used in this work are the property of Sparos Lda., and/or third-parties who have established data transfer agreements (DTAs) with Sparos Lda.

Acknowledgments: We would like to thank Vander Bruno dos Santos (Instituto de Pesca/APTA/SAA, Brazil) by kindly sharing detailed data on the experiment carried out by him and other authors on the performance of different Nile tilapia strains.

Conflicts of Interest: F.M.R.C.S., A.M.D.N., A.I.G.R., R.C.P.M., L.E.C.C. and T.S.S. work for Sparos Lda. The other authors declare that they have no conflicts of interest. The views expressed in this work are the sole responsibility of the authors and do not necessarily reflect the views of any third party. The funders had no role in the design of the study, in the collection, analyses, or interpretation of data, in the writing of the manuscript, or in the decision to publish the results.

Appendix A.

Appendix A.1. High-Level Overview of the FEEDNETICS Model

Conceptually, the model can be subdivided in two large components: a *fish model* and a *farm model*. Most of the complexity of the overall FEEDNETICS model is related to the *fish model*, which is the focus here. The roles of the *farm model* are mostly population management (e.g., deterministically remove fish in order to replicate a given time-dependent mortality rate), feeding regime management (e.g., scale given feed according to how many fish exist) and the calculation of secondary outputs (e.g., performance measures, environmental impact measures, economic indicators). All other calculations are performed within the *fish model*, which considers a set of mass pools representing different metabolites in different body compartments (in the current version: gut, blood, and body) and different states, along with a set of mass flows representing different biological processes (digestion, absorption, conversion, synthesis, degradation, oxidation) along with their time-dependent rates. Mathematically, the *fish model* can be seen as a set of ordinary difference equations, which are, in practice, numerically solved in the Powersim Studio 10 Expert software (Powersim Software AS, Nyborg, Norway) using the “forward Euler” integration approximation with a fixed timestep of 0.01 days (i.e., in a general sense, the model follows the dynamics of an externally-driven deterministic system of first-order ordinary difference equations, in practice).

A diagram detailing the overall high-level structure of the FEEDNETICS model (*fish model* and *farm model*) can be seen in Figure A1.

Unless stated otherwise, the use of the “FEEDNETICS model” throughout the rest of this appendix refers specifically to the *fish model* part of the general model.

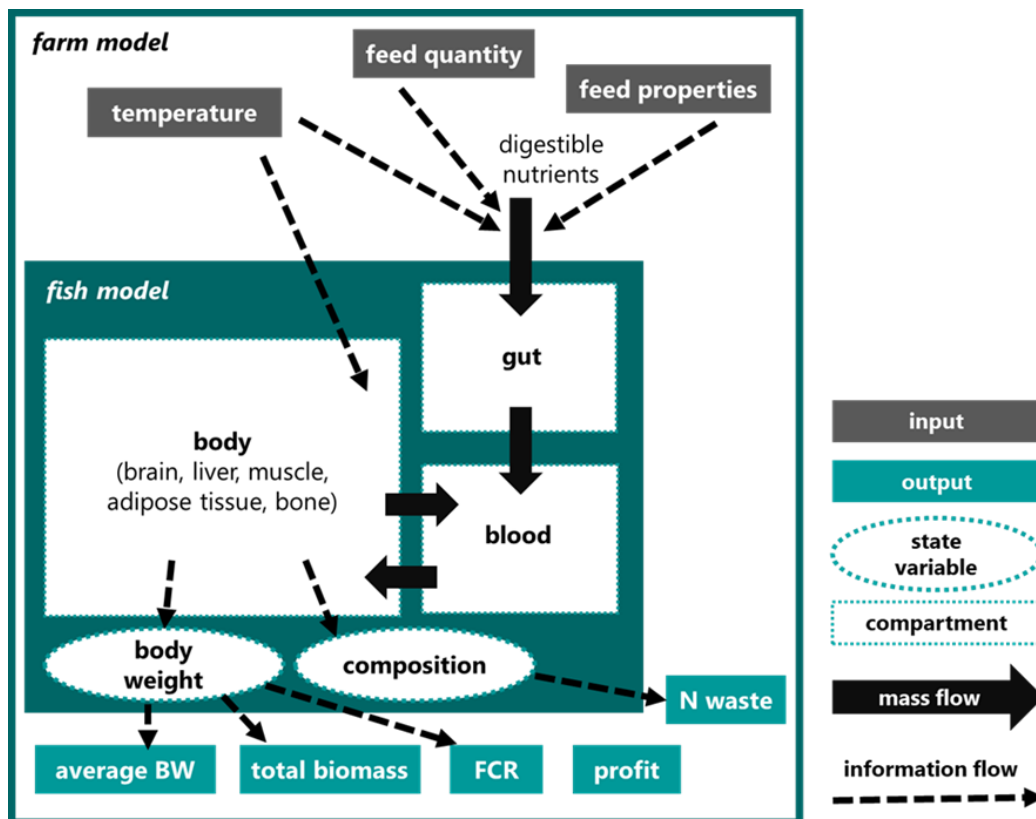


Figure A1. Diagram detailing a simplified high-level structure of FEEDNETICS, with emphasis on the *fish model* component. Inputs to the *fish model* (previously pre-processed by the *farm model*) drive its time-dependent behavior, while its state variables are used in the calculation of all outputs (only a small subset of which are depicted in the diagram). Each compartment contains a set of mass pools (not depicted) which represent the amount of each metabolite in each compartment.

Appendix A.2. Model Inputs

Given that the behavior of the model is strongly driven by its inputs, it is important to consider them as a starting point. The FEEDNETICS model can be seen as driven by basically three time-dependent inputs, all with a time resolution of 0.01 days:

1. Temperature (°C), single value. In practice, the user provides “daily temperature average” and “daily temperature amplitude” and a typical daily temperature curve is generated by the *farm model* using a sinusoidal shape, assuming that the lowest temperature occurs around midnight.
2. Feed given (g/day), single value. In practice, the user provides either this information on a daily resolution level or a feeding table (matrix defining the feeding rates, expressed as % body weight/day, per fish body weight class and temperature class) from which this information is estimated on a daily resolution level. The daily given feed is then distributed along the day using information on the frequency and distribution of meals (i.e., number of meals, time of first meal, and time between meals).
3. Feed properties, many values (often constant along time). These are:
 - Macronutrient composition (i.e., crude protein, crude lipids, ash, fiber, gross energy, phosphorus);
 - Apparent digestibility coefficients (ADCs; i.e., crude protein, crude lipids, gross energy, phosphorus);
 - Amino acid profile (i.e., the standard 20 proteinogenic amino acids);
 - Fatty acid profile (i.e., 20 different fatty acids).

Appendix A.3. Feed Intake Control and Gut Compartment

Regarding feed intake control, the FEEDNETICS model follows the modelling approach of Lupatsch [41], with some adaptations:

$$FI_{max} = a \times BW^b \times e^{cT} \times I(T > T_{low}) \times I(T < T_{high}), \quad (A1)$$

where FI_{max} represents maximum feed intake in grams/day, a , b , c , T_{low} , and T_{high} are species-specific parameters, BW represents fish body weight in grams, T represents the current temperature, and I represents the indicator function (returns 1 if the comparison is true and 0 if the comparison is false).

This implies that the maximum feed intake is assumed to depend linearly on a power of the body weight and exponentially on temperature, being reduced to zero if temperature is too low or too high. This step (among others) attempts to induce the loss of weight observed in fish under extreme temperatures, which is not seen for high temperatures, if strictly following the feed intake model suggested by Lupatsch [41].

To prevent discontinuities in the model (which can make model optimization more challenging), we adopt an analytical approximation of the above expression (which converges to the above expression as the parameter β tends to infinity):

$$FI_{max} = a \times BW^b \times e^{cT} \times \frac{1}{1 + \left(\frac{T_{low}}{T}\right)^\beta} \times \frac{1}{1 + \left(\frac{T}{T_{high}}\right)^\beta}. \quad (A2)$$

As such, actual feed intake is then calculated as:

$$FI = \min(FI_{max}, feed\ given), \quad (A3)$$

Taking into account the actual feed intake, along with the (possibly time-dependent) feed composition and apparent digestibility coefficients (ADCs), the amount of digestible nutrients being introduced in the *gut* compartment is calculated. The presence of indigestible nutrients in the gastrointestinal tract is not explicitly modeled in FEEDNETICS,

though these values (along with wasted/non-ingested feed) are tracked for the purpose of environmental impact estimation.

At this point, the mass of ingested feed is converted to molar amounts of nutrients:

$$DI_{nutrient} = \frac{FI \times ADC_{nutrient} \times feed_{nutrient}}{Mw_{nutrient}}, \tag{A4}$$

where $DI_{nutrient}$ represents the digestible intake of a nutrient per unit of time, $ADC_{nutrient}$ is the given apparent digestibility coefficient of the nutrient, $feed_{nutrient}$ is the percentage of the nutrient in the feed, and $Mw_{nutrient}$ is the molecular weight of the nutrient.

To model digestion and absorption rates ($digestion_{nutrient}$ and $absorption_{nutrient}$, respectively) of ingested feed, we considered a simplified model with a single enzyme that converts digestible nutrients ($digestible_{nutrient}$) to digested nutrients ($digested_{nutrient}$), then a single receptor/transporter that converts digested nutrients to absorbed nutrients, using second-order kinetics, as follows:

$$digestion_{nutrient} = k_{digestion} \times enzyme \times digestible_{nutrient}, \tag{A5}$$

$$absorption_{nutrient} = k_{absorption} \times receptor \times digested_{nutrient}, \tag{A6}$$

where the $k_{digestion}$ and $k_{absorption}$ rate constants, and $enzyme$ and $receptor$ indicate their abundance.

To model enzyme and receptor abundance, we considered simple first-order processes, where enzyme/receptor production is proportional to substrate abundance, while enzyme/receptor degradation is proportional to enzyme/receptor abundance.

$$\frac{d(enzyme)}{dt} = \left(k_{enz_prod} \times \sum_{nutrient} digestible_{nutrient} \right) - k_{enz_deg} \times enzyme, \tag{A7}$$

$$\frac{d(receptor)}{dt} = \left(k_{rec_prod} \times \sum_{nutrient} digested_{nutrient} \right) - k_{rec_deg} \times receptor, \tag{A8}$$

where k_{enz_prod} and k_{enz_deg} are rates of enzyme production and degradation, respectively, and k_{rec_prod} and k_{rec_deg} are rates of receptor production and degradation, respectively.

The *gut* compartment does not effectively affect nutrient digestibility (since ADCs are provided as input), but simply delays the availability of ingested nutrients for metabolic processes (anabolism or catabolism).

A diagram representing the internal structure of the *gut* compartment, with all the considered mass pools and mass flows, can be seen in Figure A2, which shows that the structure is generally linear and one-way.

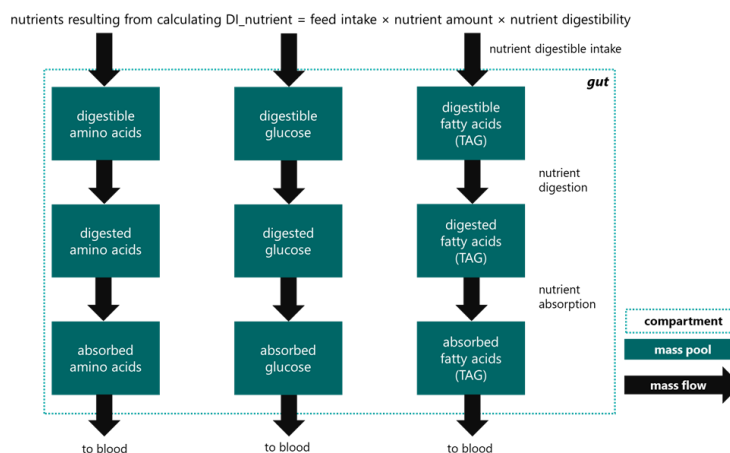


Figure A2. Diagram detailing the internal structure of the *gut* compartment, showing the different pools considered, along with mass flows between pools. For simplicity, the amino acid and fatty acid

pools are displayed in vectorized form (i.e., they appear as a single unit, but actually represent 20 different pools each).

Additionally, a set of calculations is performed to provide the fish with information on short-term feeding history. The result is two variables between 0 and 1 (“fed” and “fasting”) that are used in other downstream calculations.

Appendix A.4. Core Metabolic Model (Blood and Body Compartments)

The FEEDNETICS model is built around a core metabolic model that represents the main anabolic and catabolic processes in fish. To ensure a simple model, all main body tissues (e.g., liver, brain, muscle) are considered under a single *body* compartment, which interfaces with the *blood* compartment. Although movement of metabolites between the *body* and *blood* compartments is two-way, mass flow tends to occur mostly in the blood-to-body direction due to the regular entry of nutrients from the gut to the bloodstream. In this model, the role of the *blood* compartment is two-fold: to deliver absorbed nutrients to the *body* compartment, delaying them, and to regulate metabolite availability for use in metabolic processes (*body* compartment).

A diagram showing the general structure of the *blood* and *body* compartments, along with the considered mass flows, can be seen in Figure A3.

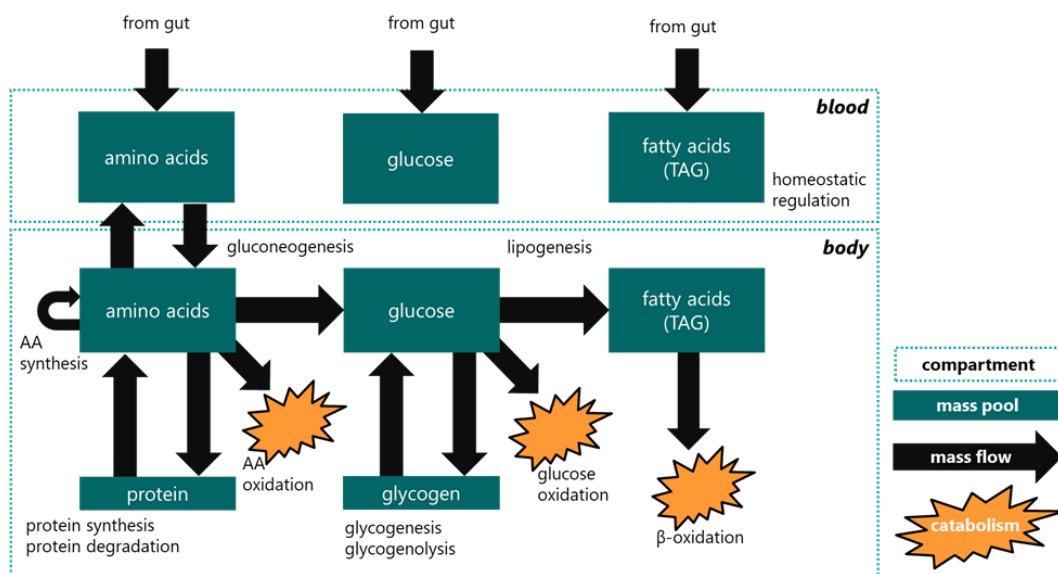


Figure A3. Diagram detailing the internal structure of the *blood* and *body* compartments, showing the different pools considered, along with mass flows between pools. For simplicity, the amino acid and fatty acid pools are displayed in vectorized form (i.e., they appear as a single unit, but actually represent 20 different pools each).

Appendix A.5. Body Weight and Composition Model

A central point of the FEEDNETICS model relates to the control of body composition. As a starting point, fish body is assumed to be mostly composed of water, crude protein (which includes protein, amino acids, and other nitrogen-containing compounds), crude lipids (fatty acids, triacylglycerides, phospholipids, steroids), and minerals/ash. The amount of glucose and glycogen is generally below 1% of whole-body weight [42] and considered negligible in FEEDNETICS, and all dietary and metabolism-derived glucose is re-directed to lipogenesis.

First, total protein ($protein_{total}$) is directly calculated (in amino acids equivalents) by adding the contributions of all amino acids (AA):

$$protein_{total} = \sum_{i=1}^{20} proteinAA_i \times AA_Mw_i, \tag{A9}$$

where $proteinAA_i$ represents the mass of the i^{th} amino acid present in the *body* protein pool and AA_Mw_i represents the molecular weight of the i^{th} amino acid.

For the components for which an explicit mass budget cannot be established (e.g., water, ash), their quantities are assumed to depend mostly on structural biomass and, as such, directly or indirectly estimated as an allometric function of $protein_{total}$.

For all other components, their quantities are calculated by summing the contributions of the different corresponding mass pools. For example, the total amount of lipids ($lipid_{total}$) is estimated as:

$$lipid_{total} = \sum_{i=1}^{20} (TAG_body_FA_i + TAG_blood_FA_i) \times FA_Mw_i, \tag{A10}$$

where $TAG_body_FA_i$ represents the mass of the i^{th} fatty acid present in the *body* lipids pool, $TAG_blood_FA_i$ represents the mass of the i^{th} fatty acid present in the *blood* lipids pool, and FA_Mw_i represents the molecular weight of the i^{th} fatty acid.

Total body mass is estimated by summing the mass of the different components, while energy density is estimated based on the amounts of protein, lipids, and total carbohydrates, using fixed coefficients.

Furthermore, an important variable (CL_q) is also calculated. This variable controls the amount of lipids that is used to produce energy (as opposed to protein), by comparing the amount of lipids present in the body with (species and body weight dependent) reference values obtained by quantile regression:

- If the amount of lipids is below the lowest reference value, $CL_q = 0$ (i.e., use protein to produce energy and not lipids);
- If the amount of lipids is above the highest reference value, $CL_q = 1$ (i.e., as far as possible, use lipids to produce energy and spare protein);
- Otherwise, it gives an intermediate value, using a reference value that depends on the “fed state” of the fish:

$$CL_q = \frac{1}{1 + \left(\frac{lipid_{ref}}{lipid_{total}}\right)^\beta}, \tag{A11}$$

where β controls the shape of the curve and $lipid_{ref}$ is calculated based on the *fasting* variable, as an interpolation between the lowest and highest reference values (i.e., when *fasting* is 0, the reference value is the maximum value; when *fasting* is 1, the reference value is the minimum value).

Appendix A.6. Energetic Model

An important aspect of the accurate modelling of fish growth is to ensure that estimates are consistent with basic physical principles, such as energy conservation. As such, we consider the following assumptions:

- Energy production and energy expenditure can be represented in ATP (adenosine triphosphate) equivalents, given that ATP is (along with other nucleoside phosphates) the most widespread energy-yielding metabolite in cells;
- During any given step (timescale ≈ 14.4 min per timestep), we assume that ATP levels are essentially in steady-state (i.e., the rate of ATP production must match the rate of ATP degradation over the course of any given timestep);

- ATP expenditure is assumed to result from a combination of:
 - Anabolism energy costs—energy expenditure due to anabolic reactions, which is implicitly defined by their rates (protein synthesis, glycogenesis, lipogenesis, non-essential AA synthesis);
 - Catabolism energy costs—energy expenditure due to energy-consuming catabolic reactions, which is implicitly defined by their rates (protein degradation);
 - Basal energy costs—fixed feed-independent costs that depend on fish body weight and temperature (and accounts for fixed costs not included in the previous two points);
 - Feeding energy costs—variable costs that depend on the fish’s “fed state” (and accounts for feed-dependent costs not included in the previous three points);
- A fixed upper limit on ATP expenditure rate is assumed ($600 \mu\text{mol.g}^{-1}.\text{h}^{-1}$), to ensure that the actual values remain within physiologically-reasonable bounds [43];
- ATP production is constrained to match ATP expenditure and results from a combination of:
 - Metabolite conversion (e.g., gluconeogenesis from AA and interconversion of AA);
 - Oxidative catabolism (glucose oxidation, beta-oxidation of fatty acids, amino acid oxidation);
- The rates of AA oxidation and FA beta-oxidation are determined by the difference between “required ATP production to match ATP expenditure” and “ATP resulting from metabolite conversion and glucose oxidation”, with the relative weight of the two catabolic processes being defined according to the CL_q variable.

A system of valves is used to ensure that ATP expenditure and ATP production always match, even in unusual situations (e.g., not enough substrate to ensure required ATP production; not enough ATP expenditure to balance out energy-yielding reactions). If we ignore this system, the resulting balances can be described as:

$$ATP_{exp} = ATP_{cost_{anab}} + (1 + fed_{scaling} \times feed_{cost_{scale}}) \times ATP_{cost_{basal}}(BW, T), \tag{A12}$$

$$ATP_{req} = ATP_{exp} - ATP_{prod_{catab}} - ATP_{prod_{glucos}}, \tag{A13}$$

where ATP_{exp} represents ATP expenditure (in mol/hr), $ATP_{cost_{anab}}$ represents ATP costs due to explicit metabolic reactions, $fed_{scaling}$ is a value between 0 and 1 that represents the fish’s fed state, $feed_{cost_{scale}}$ is a parameter that controls feeding costs, $ATP_{cost_{basal}}$ represents (otherwise unaccounted) basal energy costs, BW is the current body weight of fish (in grams), T is the current temperature (in °C), ATP_{req} represents the required ATP from amino acid oxidation and fatty acid beta-oxidation, $ATP_{prod_{catab}}$ represents the ATP produced by energy-yielding metabolite conversion reactions, and $ATP_{prod_{glucos}}$ represents the ATP production due to glucose oxidation.

The remaining ATP requirements (ATP_{req}) are met using a combination of amino acid oxidation and fatty acid beta-oxidation that is controlled by the CL_q variable. The way to interpret this variable (which is bounded between 0 and 1) is as the ratio between “mass of lipid oxidized” and “total mass of protein + lipid oxidized”.

$$m_{oxAA} = \frac{1 - CL_q}{CL_q} m_{oxFA}, \tag{A14}$$

$$ATP_{req} = m_{oxAA} \times ATP_{stoich_{AA}} + m_{oxFA} \times ATP_{stoich_{FA}}, \tag{A15}$$

$$m_{oxAA} = \frac{ATP_{req}}{\frac{CL_q}{1-CL_q} ATP_{stoich_{FA}} + ATP_{stoich_{AA}}}, \tag{A16}$$

where m_{oxAA} represents the rate of amino acid oxidation, m_{oxFA} represents the rate of fatty acid beta-oxidation, and $ATP_{stoich_{AA}}$ and $ATP_{stoich_{FA}}$ represent the profile-dependent

ATP yield of the catabolic reactions (in mol ATP/g fuel) for amino acids and fatty acids, respectively.

The value of m_{oxAA} therefore provides an estimate of the required mass of amino acids to be oxidized. On the other hand, it is important to ensure that the consumption of amino acids complies with the minimum protein requirements (see below Appendix A.7. Nitrogen metabolism—amino acids and proteins). As such, the actual value used is calculated as such:

$$m_{oxAA} = \max\left(\frac{ATP_{req}}{\frac{CL_q}{1-CL_q} ATP_{stoch_{FA}} + ATP_{stoch_{AA}}}, \min_AA_loss\right), \quad (A17)$$

where \min_AA_loss is calculated as detailed below (in the Appendix A.7. Nitrogen metabolism—amino acids and proteins).

The actual rate of required fatty acid beta-oxidation is then calculated as:

$$m_{oxFA} = \frac{ATP_{req} - ATP_{AA_{ox}}}{ATP_{stoch_{FA}}}, \quad (A18)$$

where $ATP_{AA_{ox}}$ represents the ATP generated from amino acid oxidation.

Appendix A.7. Nitrogen Metabolism—Amino Acids and Proteins

Perhaps the most important aspects of FEEDNETICS have to do with how it deals with nitrogen metabolism (namely, protein synthesis and degradation, as well as amino acid interconversion and oxidation). The current implementation of protein synthesis and degradation processes are heavily inspired by the ones described in the models developed by Conceição et al. [6] and Bar et al. [23,27,44], and the mainstream literature on amino acid metabolism in fish [45–47] and other vertebrates [48,49]. It assumes a fixed (species-specific) amino acid profile (i.e., the rates of accumulation and loss of amino acids from the protein pool relative to each other are constant).

Appendix A.7.1. Protein Synthesis

Regarding protein synthesis, first, a maximum rate of protein synthesis (\max_prot_{synth}) is calculated using a simplified version of Bar et al. [23,27,44] protein synthesis model which assumes a fixed amino acid profile for the synthesized protein:

$$\max_prot_{synth} = \min\left(kRNA \times vs_T \times Cs \times protein_{total}, \lim_prot_{synth}\right), \quad (A19)$$

where \lim_prot_{synth} represents the maximum rate of protein synthesis in terms of available substrate (i.e., free amino acids), $kRNA$ represents translation rate, vs_T represents the temperature effect on protein synthesis, and Cs represents the transcription rate (i.e., quantity of RNA present per gram of protein).

The calculation of the temperature effect on protein synthesis (vs_T) is straightforward, since it assumes a linear model:

$$vs_T = temperature_{effect} \times T, \quad (A20)$$

where $temperature_{effect}$ is a scalar parameter and T is the current temperature (in °C).

The calculation of $kRNA$ aims to emulate the effects of ribosome occupancy on the limitation of protein synthesis. First, ribosomes are assumed to exist in two states: occupied ($ribo_{occupied}$) or unoccupied ($ribo_{unoccupied}$). Then, the transitions between the two states are calculated as such:

$$ribo_{activation} = k_{ribo} \times ribo_{occupied} \times valve_{activation}, \quad (A21)$$

$$ribo_{deactivation} = k_{ribo} \times ribo_{unoccupied} \times valve_{deactivation}, \quad (A22)$$

$$\frac{d}{dt}(ribo_{occupied}) = ribo_{deactivation} - ribo_{activation}, \tag{A23}$$

$$\frac{d}{dt}(ribo_{unoccupied}) = ribo_{activation} - ribo_{deactivation}, \tag{A24}$$

where k_{ribo} is a time constant, while $valve_{activation}$ and $valve_{deactivation}$ are values between 0 and 1 that control the balance between the two states. $valve_{activation}$ is close to 1 if the fat levels are above the reference values and if free amino acids are also above their reference values (and closer to 0 otherwise), while $valve_{deactivation}$ is closer to 1 the closer actual protein synthesis rate approaches the maximum protein synthesis rate (serving as a negative feedback regulation signal).

Total ribosome activity ($ribo_{act}$; as a value between 0 and 1) is then estimated and used to interpolate (linearly, on a log-scale) between two constants ($kRNA_{min}$ and $kRNA_{max}$), as such:

$$ribo_{act} = \frac{ribo_{unoccupied}}{ribo_{occupied} + ribo_{unoccupied}}, \tag{A25}$$

$$kRNA = e^{(1-ribo_{act}) \times \ln(kRNA_{min}) + ribo_{act} \times \ln(kRNA_{max})}. \tag{A26}$$

After determining the maximum rate of protein synthesis, two valve values (i.e., values between 0 and 1) are calculated: $prot_{synt_{regulator}}$ and $AA_{synt_{valv}}$. The first one suppresses protein synthesis in situations of prolonged fasting and whenever lipid levels are abnormally low (thus inducing an increase in de novo lipid synthesis):

$$prot_{synt_{regulator}} = 0.05 + 0.95 \times \min(1, \max(0, CL_q + fed - starving)), \tag{A27}$$

while the second one suppresses protein synthesis according to how low the free amino acid levels are (according to their set reference levels):

$$AA_{synt_{valv}} = \min \left(\frac{1}{1 + \frac{1}{\left(\frac{AA_{free}}{refAA_{free}} \right)^{AA_{synt_{beta}}}}} \right), \tag{A28}$$

where $\min()$ is a function that accepts a vector as input and returns a scalar (the minimum) as output, AA_{free} is a vector containing the free amount of each amino acid, $refAA_{free}$ is a vector containing the reference values for the free amount of each amino acid, and $AA_{synt_{beta}}$ is an exponent that modifies the valve behavior.

The actual rate of protein synthesis is then calculated as a product of these factors, being afterwards converted into amino acids equivalents using a fixed species-dependent amino acid profile:

$$A_{prot_{synth}} = max_prot_{synth} \times prot_{synt_{regulator}} \times AA_{synt_{valv}}. \tag{A29}$$

Appendix A.7.2. Protein Degradation

Regarding protein degradation, it is also assumed to follow a fixed amino acid profile (i.e., when protein is converted into amino acids, it follows the same amino acid profile as used for amino acid synthesis to ensure that the total amino acid profile of the fish approximates the set profile). First, the upper bound for protein degradation ($max_{prot_{deg}}$) is calculated and assumed to be proportional to the total amount of protein:

$$max_{prot_{deg}} = k_{deg} \times deg_{temp_{factor}} \times protein_{total}, \tag{A30}$$

where k_{deg} represents a scaling factor and $deg_{temp_{factor}}$ represents the quadratic effect of temperature on protein degradation:

$$deg_{temp_{factor}} = Vd_b + Vd_m \times (temperature - T_{optimal})^2, \tag{A31}$$

where Vd_b , Vd_m , and $T_{optimal}$ control the shape of the parabola.

The lower bound for protein degradation ($min_{prot_{deg}}$) is calculated assuming that it is proportional to the protein requirements:

$$min_{prot_{deg}} = prot_{deg_min_factor} \times min_AA_loss, \tag{A32}$$

where min_AA_loss is defined below by equation (A35).

Finally, a valve value is calculated and used to interpolate between the two bounds, based on the available amounts of free amino acids:

$$AA_{deg_{valv}} = \min\left(\frac{1}{1 + \left(\frac{AA_{free}}{refAA_{free}}\right)^{AA_{deg_beta2}}}\right)^{AA_{deg_beta1}}, \tag{A33}$$

where $\min()$ is a function that accepts a vector as input and returns a scalar (the minimum) as output, while AA_{deg_beta1} and AA_{deg_beta2} control the shape of the response. The actual rate of protein degradation ($prot_{deg}$) is then calculated, being afterwards converted into amino acid equivalents using a fixed species-dependent amino acid profile:

$$prot_{deg} = min_{prot_{deg}} + (max_{prot_{deg}} - min_{prot_{deg}}) \times AA_{deg_{valv}}. \tag{A34}$$

Appendix A.7.3. Amino Acid Oxidation

Regarding amino acid oxidation, it is assumed that there is a basal amino acid oxidation rate that follows the same logic as the “protein fasting maintenance” calculations of Lupatsch [41]:

$$min_AA_loss = req_prot_a \times e^{req_prot_b \times temperature} \times \left(\frac{bw}{1000}\right)^{req_prot_c}, \tag{A35}$$

Where req_prot_a , req_prot_b , and req_prot_c are parameters describing the effects of temperature and body weight on protein fasting maintenance.

The total amount of amino acids oxidized (m_{oxAA}) is then calculated, as detailed in the Appendix A.6. Energetic model above, and distributed by the different amino acids such that those that exist in higher amounts (in relation to their reference values) are preferably used. First, two auxiliary vector quantities are calculated:

$$AA_{free_max_norm} = \frac{AA_{free}}{max_refAA_{free}}, \tag{A36}$$

$$AA_{free_min_norm} = \frac{AA_{free}}{min_refAA_{free}}, \tag{A37}$$

and then they are combined as such:

$$AA_{ox_{valv}} = \min\left(\frac{AA_{free_max_norm}}{\sum AA_{free_max_norm}}, \frac{AA_{free_min_norm}}{\sum AA_{free_min_norm}}\right), \tag{A38}$$

and normalized to ensure that resulting vector is a partition:

$$AA_{ox_{weights}} = \frac{AA_{ox_{valv}}}{\sum AA_{ox_{valv}}}. \tag{A39}$$

The resulting rate of amino acid oxidation is then calculated as:

$$AA_{oxrate} = AA_{oxweights} \times m_{oxAA}. \tag{A40}$$

Appendix A.7.4. Gluconeogenesis

Regarding gluconeogenesis (i.e., synthesis of glucose from amino acids), first, a maximum overall rate of glucose synthesis from amino acids ($V_{maxgluconeo}$) is calculated, assuming an exponential effect of temperature and a linear effect of body weight, and having into account possible substrate limitations:

$$V_{maxgluconeo} = \min \left(AA_{glucoweights} \times stoich_{glucose AA \rightarrow glucose} \times a_{gluconeo} \times bw \times e^{b \times temperature}, stoich_{glucose AA \rightarrow glucose} \times \frac{AA_{free}}{timestep} \right) \tag{A41}$$

where $AA_{glucoweights}$ is a partitioning vector (similar to $AA_{oxweights}$) that ensures that gluconeogenesis is suppressed, unless there are abundant amino acids, and $a_{gluconeo}$ and b are parameters.

The actual rate of gluconeogenesis ($V_{gluconeo}$) is then calculated by having into account an inhibiting effect of glucose on its synthesis (negative feedback) and ensuring that abundant amino acids are given preference as substrates:

$$V_{gluconeo} = V_{maxgluconeo} \times \frac{1}{1 + \frac{glucose}{ref_{glucose}}} \times AA_{glucoweights}. \tag{A42}$$

Appendix A.7.5. Synthesis of Non-Essential Amino Acids

Regarding the synthesis of non-essential amino acids, reactions are simulated with stoichiometries recalculated to assume glucose as a source of carbon and ensuring that the nitrogen balance is not violated (i.e., the amount of nitrogen incorporated into synthesized amino acids is upper bounded by the amount of nitrogen lost during that timestep, from, for example, amino acid oxidation). For the stoichiometries, it uses mostly the work of Olsen [50] as an information source. Here, reactions are separated into “ATP-producing” and “ATP-consuming”, but are calculated in a similar way, using matrix operations. The formulas ensure that the reactions are stimulated by glucose (substrate) and suppressed by the products of the reactions. In a similar way, reaction rates for the conversion of methionine in cysteine and of phenylalanine in tyrosine are also calculated.

Appendix A.8. Carbon Metabolism—Glucose, Glycogen, and Fatty Acids

Besides nitrogen metabolism, it is important to also accurately model central (carbon) metabolism, which encompasses the metabolism of carbohydrates (glucose and glycogen) and lipids (as fatty-acid equivalents).

Appendix A.8.1. Glucose Oxidation

Regarding glucose oxidation, first, a maximum value ($V_{maxglucox}$) is calculated, having into account substrate availability:

$$V_{maxglucox} = \min \left(a_{glucox} \times bw \times e^{b \times temperature}, \frac{glucose}{timestep} \right). \tag{A43}$$

Then, two valves are applied to ensure that glucose oxidation is suppressed whenever glucose levels become particularly low and whenever energy availability is too high.

Appendix A.8.2. Glycogenesis and Glycogenolysis

Regarding glycogenesis (i.e., synthesis of glycogen from glucose) and glycogenolysis (i.e., degradation of glycogen into glucose), they are both calculated based on a common maximum rate ($V_{\max\text{glycogen}}$) proportional to the total amount of body protein:

$$V_{\max\text{glycogen}} = \text{constant} \times \text{protein}_{\text{total}}. \quad (\text{A44})$$

This value is then used to calculate the reaction rate, assuming Michaelis-Menten-like kinetics, and taking, in the case of glycogenesis, glucose as a stimulant and glycogen as an inhibitor, and, in the case of glycogenolysis, glycogen as a stimulant and glucose as an inhibitor.

Appendix A.8.3. Lipogenesis

Regarding lipogenesis (i.e., synthesis of lipids from glucose), first, a maximum lipogenesis rate ($V_{\max\text{lipogen}}$) is calculated:

$$V_{\max\text{lipogen}} = \min\left(a_{\text{lipogen}} \times bw \times e^{b \times \text{temperature}}, \frac{\text{glucose}}{\text{timestep}}\right). \quad (\text{A45})$$

Then, additional factors are added to ensure that lipogenesis is suppressed when glucose becomes unavailable and when lipid levels become abnormally high.

Appendix A.8.4. Beta-Oxidation

Regarding the rate of beta-oxidation (i.e., oxidation of fatty acids), it is defined based on the m_{oxFA} value, calculated as detailed in the above Appendix A.6. Energetic model, multiplied by the absolute availability of the different fatty acids (i.e., it assumes a pure dilution model: all fatty acids enter the body in the proportion they exist in the diet and they are lost in the proportion they exist in the body):

$$\text{TAG}_{\text{betox}} = \text{TAG}_{\text{oxweights}} \times m_{\text{oxFA}}. \quad (\text{A46})$$

Appendix B.

In this appendix, we present some additional use cases that illustrate the potential application of the FEEDNETICS model to support the industry to: (i) evaluate the impact of different commercial feeds; (ii) evaluate the impact of different temperature profiles; and (iii) predict the long-term effects of marginal changes in diet digestibility.

Use case 1: Evaluate the impact of different commercial feeds on trout production performance

Use case 1 illustrates how FEEDNETICS can be used to evaluate the impact of two high energy feeds on rainbow trout production performance, and to quantify savings on feed obtained by the best performing scenario. This use case was set up for a generic RAS farm and two commercial feeds used by the rainbow trout RAS industry were considered. The key results and outcomes are presented in Figure A4 and are only applicable to the input data specified. Changes in rearing temperature, feed properties, feeding rates, and target harvest weight will alter results and main outcomes. In this case, the main outcomes identify Aquafeed 1 as leading to an overall better performance, including a significant decrease in the total N and P wastes, as well significant better economic conversion (Figure A4). This information is highly relevant for optimizing RAS production as it implies a balance between fish growth, feed efficiency, water quality, and profitability. Evaluating feeding efficiency indicators is very important, not only for feed conversion economics, but also for planning and managing the biofilter.

Use case | Evaluate the impact of different RAS feeds on trout production performance



Rainbow trout

OBJECTIVE

Evaluate the performance of rainbow trout fed two high-energy feeds used by the RAS industry, and quantify savings on feed, considering a harvest weight of 1 kg.

INPUT DATA

Production conditions

Initial weight **50 g**
 Initial nr. of fish **15,000**
 Mortality **1 % per month**
 Feed waste **0 %**
 Water temperature **~13 °C** (11 °C to 16 °C)



Feeding regime

- Aquafeed 1 is denser in nutrients, with higher digestible protein and lipids levels, targeting a reduced FCR.

- Improvements (Aquafeed 1) come at a higher cost (+6%).

	Aquafeed 1			Aquafeed 2		
Feed cost (% variation)	+6%			ref		
Proximate composition	3mm	4.5mm	6mm	3mm	4.5mm	6mm
Digestible protein (%)	41.6	40.5	35.2	38.6	37.0	33.9
Digestible lipids (%)	26.9	28.7	29.7	23.5	25.4	27.1
Digestible energy (MJ/kg)	22.4	22.6	22.8	21.1	21.4	21.9
DP/DE (g/MJ)	18.5	17.9	15.4	18.3	17.3	15.5
Digestible phosphorus (%)	0.6	0.6	0.5	0.8	0.7	0.6
Ash (%)	5.2	5.4	4.3	7.0	6.0	6.0
Fiber (%)	2.0	2.0	2.0	2.1	2.1	2.1
Amino acid profile	Default rainbow trout feed					
Fatty acid profile	Default rainbow trout feed					
Feed ration	Same feeding table					

PREDICTION OUTPUTS

Growth prediction

- Aquafeed 1 allows fish to reach the target weight (1 kg) 36 days earlier.



Performance at 1 kg

	Aquafeed 1	Aquafeed 2
Days in production	261	297
Growth rate (% BW per day)	1.16	1.01
FCR	1.05	1.21
Economic conversion ratio (€ feed/kg biomass gain)	1.08	1.18
Cumulative feeding (ton)	13.7	15.6
Total N waste (kg N/ton biomass gain)	41	49
Total P waste (kg P/ton biomass gain)	3.4	5.8

Savings on feeding (€ per ton of fish produced) 100

MAIN OUTCOMES

The FEEDNETICS model predicts that **Aquafeed 1 leads to a better performance: shorter (12%) production cycle, improved FCR by 0.16 units, and decreased total N and P waste of about -17% and -43%, respectively**, when compared with the other high-energy feed. Aquafeed 1 better performance translates in **savings on feed of about 100 € per ton of fish produced**, despite its higher unit cost.

Figure A4. Use case 1: Evaluate the impact of different RAS feeds on trout production performance. All results are FEEDNETICS model predictions.

Use case 2: Evaluate the impact of different temperature profiles on post-smolt production performance

Use case 2 illustrates how FEEDNETICS can be used to evaluate post-smolt salmon performance produced in sites with different temperature profiles, including controlled temperature conditions, as can be found in recirculating aquaculture systems (RAS). This is a relevant topic for the salmon industry, as post-smolt production (up to 1 kg) has become more common to shorten time in sea cages [51]. In particular, this use case was set up to reproduce the Atlantic salmon (*Salmo salar*) growth data obtained from a semi-commercial scale research work [52] upscaled to a 1 million post-smolt operation, considering two different temperature scenarios: (i) yearly temperature profile at Ålesund, Norway (data from seatemperature.org), and (ii) a constant average temperature of 13.4 °C to represent the conditions in a RAS system and match the post-smolt rearing conditions described by Crouse et al. [52] for Cohort B2. The key results and outcomes are presented in Figure A5.

In addition to evaluating different temperature profiles, this use case can be further developed and customized considering:

- Different feeds and feeding rates used (or planned) for RAS and cage operations;
- Production costs, besides feed costs, and the fish price, for RAS and cage operations;
- Different mortality rates for RAS and cage operations.

These different data inputs will impact not only the predicted fish performance but also the model output indicators for production profitability. They can be inserted into FEEDNETICS according to each user's specific farming conditions in order to perform a cost-benefit analysis on producing post-smolts in RAS up to larger sizes before moving fish to sea cages.

Use case | Evaluate the impact of different temperatures on post-smolt production performance



Atlantic salmon

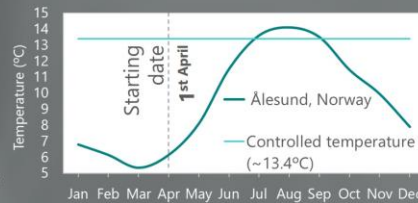
OBJECTIVE

Evaluate the performance of post-smolts produced in sites with different temperature profiles, including controlled temperature conditions (as can be found in RAS), considering a target weight of 1 kg.

INPUT DATA

Production conditions

Initial weight **105 g**
 Initial nr. of fish **1,100,000**
 Mortality **1.3 % per month**



2 different temperature scenarios

Feeding regime

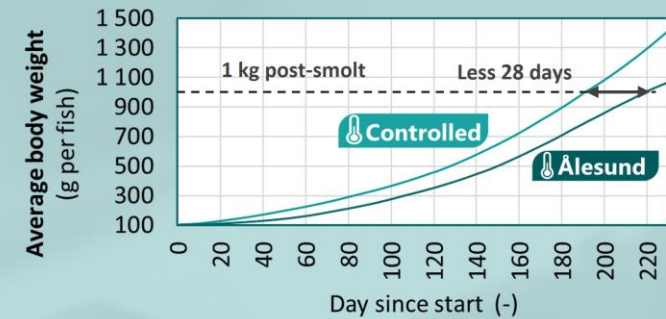
- The same feed and feeding table were considered for the 2 temperature scenarios.
- Alternatively, users can choose different feeding regimes for the controlled temperature scenario.

Proximate composition	Commercial feed	
	4.5mm	6mm
Digestible protein (%)	40.5	35.9
Digestible lipids (%)	24.0	29.6
Digestible energy (MJ/kg)	20.9	22.2
DP/DE (g/MJ)	19.4	16.2
Digestible phosphorus (%)	0.8	0.8
Ash (%)	7.9	6.6
Fiber (%)	1.1	1.1
Amino acid profile	Default salmon feed	
Fatty acid profile	Default salmon feed	
Feed ration	Feeding table	

PREDICTION OUTPUTS

Growth prediction

- The controlled temperature of 13.4°C allows fish to reach the target weight (1 kg) 28 days earlier, compared with the temperature profile in Ålesund.



Performance at 1 kg

	Ålesund	Controlled
Days in production	219	191
Growth rate (% BW per day)	1.04	1.19
FCR	0.87	0.87
Economic conversion ratio (€ feed/kg biomass gain)	1.36	1.36
Cumulative feeding (ton)	777	784
Total N waste (kg N/ton biomass gain)	28	27
Total P waste (kg P/ton biomass gain)	4.4	4.4

MAIN OUTCOMES

For the production conditions considered, the FEEDNETICS model predicts that **rearing post-smolts at a controlled temperature of 13.4°C allows fish to reach 1 kg 28 days faster than in the Ålesund temperature profile.** In this simplified use case, both temperature scenarios lead to same feed and economic conversion. User specific applications can be run considering different feeding regimes, cost of operations, and different mortality rates, in order to perform a complete cost-benefit analysis on producing post-smolts up to larger sizes in RAS before moving fish to sea cages.

Figure A5. Use case 2: Evaluate the impact of different temperature profiles on post-smolt production performance. All results are model predictions.

Use case 3: Predict the long-term effects of marginal changes in diet digestibility on bream production performance

Use case 3 illustrates how FEEDNETICS can be used to complement trials that test, for example, the effects of digestibility enhancers such as lipid emulsifiers, phyto-genetic additives, gut health promoters, and feed enzymes. Due to the particularity of such trials, where most rearing conditions are controlled to be within optimal levels, and the fact that the effects of improved digestibility are not non-linear over the long-term, translating the better performance induced by digestibility enhancers to the commercial scale cannot be simply done by linear upscaling. In this regard, the use of nutrient-based models, such as FEEDNETICS, may be useful in allowing to extrapolate the long-term impact of digestibility enhancers on commercial-scale settings.

This use case was set up considering a feed additive inclusion at low level (0.2%), with minor revisions to feed formulations in order to maintain feed price. The main differences considered in the diet with the additive, compared to the baseline diet, were a marginal increase of approximately 1.5% in the apparent digestibility of crude protein, crude lipids, and gross energy. The production conditions followed typical seabream cage production settings, reared in a warm water temperature profile from Madeira Island in Portugal. The main results and outcomes are presented in Figure A6.

Use case | Predict the long-term effects of marginal changes in diet digestibility on bream production performance



Gilthead seabream

OBJECTIVE

Extrapolate for a full-production cycle the impact of digestibility improvements due to the inclusion of a feed additive and evaluate the effects on the production performance of seabream harvested at 450 g.

INPUT DATA

Production conditions



Initial weight **10 g**
 Initial nr. of fish **150,000**
 Mortality **1 % per month**
 Feed waste **12 %**



Feeding regime

Baseline: commercial seabream feed

Feed with additive inclusion at 0.2%, partially replacing fish oil.

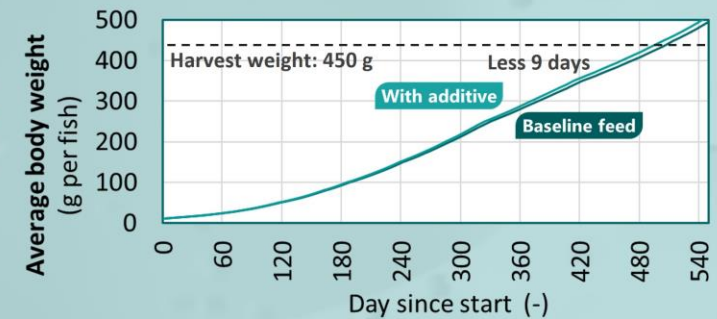
Same feed price and feeding table.

Proximal composition	Baseline feed			With additive		
	3 mm	4.5 mm	6.5 mm	3 mm	4.5 mm	6.5 mm
Crude protein (%)	47.0	45.0	42.0	47.0	45.0	42.8
Crude lipids (%)	13.0	14.0	16.0	12.8	13.8	15.8
Ash (%)	8.0	8.0	8.0	8.0	8.0	8.0
Fiber (%)	4.0	4.0	4.1	4.0	4.0	4.1
Phosphorus (%)	1.1	1.1	1.0	1.1	1.1	1.0
Gross energy (MJ/kg)	20.4	20.5	20.9	20.3	20.4	20.8
Digestibility coefficients						
Crude protein (%)	81.1	81.1	81.2	82.3	82.3	82.4
Crude lipids (%)	90.0	90.0	90.0	+1.5%	91.4	91.4
Gross energy (%)	86.7	86.7	86.4	88.0	88.0	87.7
Amino acid profile	Default gilthead seabream feed					
Fatty acid profile	Default gilthead seabream feed					

PREDICTION OUTPUTS

Growth prediction

- The marginal digestibility improvement allows fish to reach the harvest weight (450 g) 9 days earlier.



Performance at 450 g

	Baseline feed	With additive
Days in production	515	506
Growth rate (% BW per day)	0.74	0.76
FCR	2.01	1.96
Economic conversion ratio (€ feed/kg biomass gain)	2.05	2.00
Cumulative feeding (ton)	117	115
Total N waste (kg N/ton biomass gain)	108	104
Total P waste (kg P/ton biomass gain)	13.4	12.9
Savings on feeding (€ per ton of fish produced)		50

MAIN OUTCOMES

The FEEDNETICS model predicts that **due to better digestibility, the feed with additive represents savings on feed of about 50 € per ton of fish produced in full production cycle**. Furthermore, the feed with additive leads to a slightly better performance with shorter production cycle (less 9 days) and an improved FCR by 0.05 units.

Figure A6. Use case 3: Predict the long-term effects of marginal changes in diet digestibility on bream production performance. All results are model predictions.

References

1. Føre, M.; Frank, K.; Norton, T.; Svendsen, E.; Alfredsen, J.A.; Dempster, T.; Eguiraun, H.; Watson, W.; Stahl, A.; Sunde, L.M.; et al. Precision fish farming: A new framework to improve production in aquaculture. *Biosyst. Eng.* **2018**, *173*, 176–193. [[CrossRef](#)]
2. Zhou, C.; Xu, D.; Lin, K.; Sun, C.; Yang, X. Intelligent feeding control methods in aquaculture with an emphasis on fish: A review. *Rev. Aquac.* **2018**, *10*, 975–993. [[CrossRef](#)]
3. Machiels, M.A.M.; Henken, A.M. A dynamic simulation model for growth of the African catfish, *Clarias gariepinus* (Burchell 1822): I. Effect of feeding level on growth and energy metabolism. *Aquaculture* **1986**, *56*, 29–52. [[CrossRef](#)]
4. Machiels, M.A.M.; Henken, A.M. A dynamic simulation model for growth of the African catfish, *Clarias gariepinus* (Burchell 1822): II. Effect of feed composition on growth and energy metabolism. *Aquaculture* **1987**, *60*, 33–53. [[CrossRef](#)]
5. Machiels, M.A.M.; Van Dam, A.A. A dynamic simulation model for growth of the African catfish, *Clarias gariepinus* (Burchell 1822): III. The effect of body composition on growth and feed intake. *Aquaculture* **1987**, *60*, 55–71. [[CrossRef](#)]
6. Conceição, L.E.C.; Verreth, J.A.J.; Versteegen, M.W.A.; Huisman, E.A. A preliminary model for dynamic simulation of growth in fish larvae: Application to the African catfish (*Clarias gariepinus*) and turbot (*Scophthalmus maximus*). *Aquaculture* **1998**, *163*, 215–235. [[CrossRef](#)]
7. Dumas, A.; France, J.; Bureau, D. Modelling growth and body composition in fish nutrition: Where have we been and where are we going? *Aquac. Res.* **2010**, *41*, 161–181. [[CrossRef](#)]
8. Lugert, V.; Thaller, G.; Tetens, J.; Schulz, C.; Krieter, J. A review on fish growth calculation: Multiple functions in fish production and their specific application. *Rev. Aquac.* **2016**, *8*, 30–42. [[CrossRef](#)]
9. Chary, K.; Brigolin, D.; Callier, M.D. Farm-scale models in fish aquaculture—An overview of methods and applications. *Rev. Aquac.* **2022**, *14*, 2122–2157. [[CrossRef](#)]
10. Springborn, R.R.; Jensen, A.L.; Chang, W.Y.B.; Engle, C. Optimum harvest time in aquaculture: An application of economic principles to a Nile tilapia, *Oreochromis niloticus* (L.), growth model. *Aquac. Res.* **1992**, *23*, 639–647. [[CrossRef](#)]
11. Mallet, J.P.; Charles, S.; Persat, H.; Auger, P. Growth modelling in accordance with daily water temperature in European grayling (*Thymallus thymallus* L.). *Can. J. Fish. Aquat. Sci.* **1999**, *56*, 994–1000. [[CrossRef](#)]
12. De Graaf, G.; Prein, M. Fitting growth with the von Bertalanffy growth function: A comparison of three approaches of multivariate analysis of fish growth in aquaculture experiments. *Aquac. Res.* **2005**, *36*, 100–109. [[CrossRef](#)]
13. Dumas, A.; France, J.; Bureau, D.P. Evidence of three growth stanzas in rainbow trout (*Oncorhynchus mykiss*) across life stages and adaptation of the thermal-unit growth coefficient. *Aquaculture* **2007**, *267*, 139–146. [[CrossRef](#)]
14. Baer, A.; Schulz, C.; Traulsen, I.; Krieter, J. Analysing the growth of turbot (*Psetta maxima*) in a commercial recirculation system with the use of three different growth models. *Aquac. Int.* **2011**, *19*, 497–511. [[CrossRef](#)]
15. Mayer, P.; Estruch, V.D.; Jover, M. A two-stage growth model for gilthead sea bream (*Sparus aurata*) based on the thermal growth coefficient. *Aquaculture* **2012**, *358*, 6–13. [[CrossRef](#)]
16. Brigolin, D.; Pastres, R.; Tomassetti, P.; Porrello, S. Modelling the biomass yield and the impact of seabream mariculture in the Adriatic and Tyrrhenian Seas (Italy). *Aquac. Int.* **2010**, *18*, 149–163. [[CrossRef](#)]
17. Føre, M.; Alver, M.; Alfredsen, J.A.; Marafioti, G.; Senneset, G.; Birkevold, J.; Willumsen, F.V.; Lange, G.; Espmark, Å.; Terjesen, B.F. Modelling growth performance and feeding behaviour of Atlantic salmon (*Salmo salar* L.) in commercial-size aquaculture net pens: Model details and validation through full-scale experiments. *Aquaculture* **2016**, *464*, 268–278. [[CrossRef](#)]
18. Nobre, A.M.; Valente, L.M.; Conceição, L.; Severino, R.; Lupatsch, I. A bioenergetic and protein flux model to simulate fish growth in commercial farms: Application to the gilthead seabream. *Aquac. Eng.* **2019**, *84*, 12–22. [[CrossRef](#)]
19. Hua, K.; Birkett, S.; De Lange, C.F.M.; Bureau, D.P. Adaptation of a non-ruminant nutrient-based growth model to rainbow trout (*Oncorhynchus mykiss* Walbaum). *J. Agric. Sci.* **2010**, *148*, 17–29. [[CrossRef](#)]
20. Cho, C.Y.; Bureau, D.P. Development of bioenergetic models and the Fish-PrFEQ software to estimate production, feeding ration and waste output in aquaculture. *Aquat. Living Resour.* **1998**, *11*, 199–210. [[CrossRef](#)]
21. Chowdhury, M.K.; Siddiqui, S.; Hua, K.; Bureau, D.P. Bioenergetics-based factorial model to determine feed requirement and waste output of tilapia produced under commercial conditions. *Aquaculture* **2013**, *410*, 138–147. [[CrossRef](#)]
22. Stavrakidis-Zachou, O.; Papandroulakis, N.; Lika, K. A DEB model for European sea bass (*Dicentrarchus labrax*): Parameterisation and application in aquaculture. *J. Sea Res.* **2019**, *143*, 262–271. [[CrossRef](#)]
23. Bar, N.S.; Sigholt, T.; Shearer, K.D.; Krogdahl, Å. A dynamic model of nutrient pathways, growth, and body composition in fish. *Can. J. Fish. Aquat. Sci.* **2007**, *64*, 1669–1682. [[CrossRef](#)]
24. Weihe, R.; Dessen, J.E.; Arge, R.; Thomassen, M.S.; Hatlen, B.; Rørvik, K.A. Improving production efficiency of farmed Atlantic salmon (*Salmo salar* L.) by isoenergetic diets with increased dietary protein-to-lipid ratio. *Aquac. Res.* **2018**, *49*, 1441–1453. [[CrossRef](#)]
25. Peres, H.; Oliva-Teles, A. Influence of temperature on protein utilization in juvenile European seabass (*Dicentrarchus labrax*). *Aquaculture* **1999**, *170*, 337–348. [[CrossRef](#)]
26. Wang, L.; Zhang, W.; Gladstone, S.; Ng, W.K.; Zhang, J.; Shao, Q. Effects of isoenergetic diets with varying protein and lipid levels on the growth, feed utilization, metabolic enzymes activities, antioxidative status and serum biochemical parameters of black sea bream (*Acanthopagrus schlegelii*). *Aquaculture* **2019**, *513*, 734397. [[CrossRef](#)]
27. Bar, N.S.; Radde, N. Long-term prediction of fish growth under varying ambient temperature using a multiscale dynamic model. *BMC Syst. Biol.* **2009**, *3*, 107. [[CrossRef](#)]

28. Rønnestad, I.; Conceição, L.E.C. Artemia protein is processed very fast in *Solea senegalensis* larvae: A dynamic simulation model. *Aquaculture* **2012**, *350*, 154–161. [CrossRef]
29. Wickham, H. Tidy Data. *J. Stat. Softw.* **2014**, *59*, 1–23. [CrossRef]
30. Hansen, N. The CMA evolution strategy: A tutorial. *arXiv* **2016**, arXiv:1604.00772. [CrossRef]
31. Dos Santos, V.B.; Silva, V.V.; de Almeida, M.V.; Mareco, E.A.; Salomão, R.A. Performance of Nile tilapia *Oreochromis niloticus* strains in Brazil: A comparison with Philippine strain. *J. Appl. Anim. Res.* **2019**, *47*, 72–78. [CrossRef]
32. Farinha, A.P.; Schrama, D.; Silva, T.; Conceição, L.E.; Colen, R.; Engrola, S.; Rodrigues, P.; Cerqueira, M. Evaluating the impact of methionine-enriched diets in the liver of European seabass through label-free shotgun proteomics. *J. Proteom.* **2021**, *232*, 104047. [CrossRef]
33. Windell, J.T.; Foltz, J.W.; Sarokon, J.A. Effect of fish size, temperature, and amount fed on nutrient digestibility of a pelleted diet by rainbow trout, *Salmo gairdneri*. *Trans. Am. Fish. Soc.* **1978**, *107*, 613–616. [CrossRef]
34. Watanabe, T.; Takeuchi, T.; Satoh, S.; Kiron, V. Digestible crude protein contents in various feedstuffs determined with four freshwater fish species. *Fish. Sci.* **1996**, *62*, 278–282. [CrossRef]
35. Kim, J.D.; Breque, J.; Kaushik, S.J. Apparent digestibilities of feed components from fish meal or plant protein based diets in common carp as affected by water temperature. *Aquat. Living Resour.* **1998**, *11*, 269–272. [CrossRef]
36. Olsen, R.E.; Ringø, E. The influence of temperature on the apparent nutrient and fatty acid digestibility of Arctic charr, *Salvelinus alpinus* L. *Aquac. Res.* **1998**, *29*, 695–701. [CrossRef]
37. Fernández, F.; Miquel, A.G.; Guinea, J.; Martínez, R. Digestion and digestibility in gilthead sea bream (*Sparus aurata*): The effect of diet composition and ration size. *Aquaculture* **1998**, *166*, 67–84. [CrossRef]
38. Fontaine, P.; Gardeur, J.N.; Kestemont, P.; Georges, A. Influence of feeding level on growth, intraspecific weight variability and sexual growth dimorphism of Eurasian perch *Perca fluviatilis* L. reared in a recirculation system. *Aquaculture* **1997**, *157*, 1–9. [CrossRef]
39. Irwin, S.; O'halloran, J.; FitzGerald, R.D. Stocking density, growth and growth variation in juvenile turbot, *Scophthalmus maximus* (Rafinesque). *Aquaculture* **1999**, *178*, 77–88. [CrossRef]
40. Aijun, M.; Chao, C.; Jilin, L.; Siqing, C.; Zhimeng, Z.; Yingeng, W. Turbot *Scophthalmus maximus*: Stocking density on growth, pigmentation and feed conversion. *Chin. J. Oceanol. Limnol.* **2006**, *24*, 307–312. [CrossRef]
41. Lupatsch, I. Factorial approach to determining energy and protein requirements of gilthead seabream (*Sparus aurata*) for optimal efficiency of production. Ph.D. Thesis, Universitäts-und Landesbibliothek, Bonn, Germany, 2004. Available online: <https://hdl.handle.net/20.500.11811/2005> (accessed on 6 January 2023).
42. Breck, J.E. Body composition in fishes: Body size matters. *Aquaculture* **2014**, *433*, 40–49. [CrossRef]
43. Norin, T.; Clark, T.D. Measurement and relevance of maximum metabolic rate in fishes. *J. Fish Biol.* **2016**, *88*, 122–151. [CrossRef] [PubMed]
44. Bar, N.S. Dynamic model of fish growth. Ph.D. Thesis, Norges teknisk-naturvitenskapelige universitet (NTNU), Trondheim, Norway, 2007.
45. Wilson, R.P. Amino acid requirements of finfish. *Amino Acids Farm Anim. Nutr.* **1994**, 377–399.
46. Mambrini, M.; Kaushik, S.J. Indispensable amino acid requirements of fish: Correspondence between quantitative data and amino acid profiles of tissue proteins. *J. Appl. Ichthyol.* **1995**, *11*, 240–247. [CrossRef]
47. Conceição, L.E.C.; Grasdalen, H.; Rønnestad, I. Amino acid requirements of fish larvae and post-larvae: New tools and recent findings. *Aquaculture* **2003**, *227*, 221–232. [CrossRef]
48. Reeds, P.J. Regulation of protein turnover. In *Animal Growth Regulation*; Campion, D.R., Hausman, G.J., Martin, R.J., Eds.; Springer: Boston, MA, USA, 1989; pp. 183–210. [CrossRef]
49. Simon, O. Metabolism of proteins and amino acids. In *Protein Metabolism in Farm Animals*; Bock, H.D., Eggum, B.O., Low, A.G., Simon, O., Zebrowska, T., Eds.; Oxford University Press: Oxford, UK, 1989; pp. 273–366.
50. Olsen, O.A.S. Structured modelling of fish physiology. Ph.D. Thesis, Norges Tekniske Høgskole (NTH), Trondheim, Norway, 1989.
51. Mowi, A.S.A. *Salmon Farming Industry Handbook*; Mowi A.S.A: Bergen, Norway, 2020.
52. Crouse, C.; Davidson, J.; May, T.; Summerfelt, S.; Good, C. Production of market-size European strain Atlantic salmon (*Salmo salar*) in land-based freshwater closed containment aquaculture systems. *Aquac. Eng.* **2021**, *92*, 102138. [CrossRef]

Disclaimer/Publisher's Note: The statements, opinions and data contained in all publications are solely those of the individual author(s) and contributor(s) and not of MDPI and/or the editor(s). MDPI and/or the editor(s) disclaim responsibility for any injury to people or property resulting from any ideas, methods, instructions or products referred to in the content.